

**UNCLASSIFIED**

**AD 4 5 7 3 4 9**

**DEFENSE DOCUMENTATION CENTER**

**FOR**

**SCIENTIFIC AND TECHNICAL INFORMATION**

**CAMEFON STATION ALEXANDRIA, VIRGINIA**



**UNCLASSIFIED**

NOTICE: When government or other drawings, specifications or other data are used for any purpose other than in connection with a definitely related government procurement operation, the U. S. Government thereby incurs no responsibility, nor any obligation whatsoever; and the fact that the Government may have formulated, furnished, or in any way supplied the said drawings, specifications, or other data is not to be regarded by implication or otherwise as in any manner licensing the holder or any other person or corporation, or conveying any rights or permission to manufacture, use or sell any patented invention that may in any way be related thereto.

4 5 7 3 4 9  
CATALOGED BY DDC  
AS AD NO. 457349

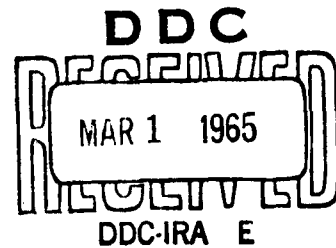
ARL-TR-64-11

DYNAMIC RESPONSE ANALYSIS OF  $+G_x$  IMPACT ON MAN

H. C. Feder  
E. H. Root

NOVEMBER 1964

6571st Aeromedical Research Laboratory  
Aerospace Medical Division  
Air Force Systems Command  
Holloman Air Force Base, New Mexico



**This report may be reproduced to satisfy needs of U. S. Government agencies. No other reproduction is authorized except with permission of the 6571st Aeromedical Research Laboratory, Holloman AFB, NMex.**

**This report is made available for study with the understanding that proprietary interests in and relating thereto will not be impaired. In case of apparent conflict or any other questions between the Government's rights and those of others, notify the Judge Advocate, Air Force Systems Command, Andrews Air Force Base, Washington, D. C. 20331.**

**Do not return this copy. Retain or destroy.**

DYNAMIC RESPONSE ANALYSIS OF  $+G_x$  IMPACT ON MAN

H. C. Feder  
E. H. Root

## FOREWORD

This study was conducted in support of Project 7231, Biomechanics of Aerospace, Task 723106, Biological Parameters of Impact. This task is assigned to the 6571st Aeromedical Research Laboratory, Holloman Air Force Base, New Mexico.

The computer program and the data reduction was supervised by Mr. F. P. Ehni, Chief of the Analog Computation Division, Air Force Missile Development Center, Holloman AFB.

This report was coordinated with the Biodynamics and Bionics Division of the 6570th Aeromedical Research Laboratories, Wright-Patterson AFB, Ohio. Following Dr. H. von Gierke's advice, particular emphasis was put on the Introduction (Section I) and the Recommendations (Section VI) to show how this study fits into the overall situation of impact research.

This technical report has been reviewed and is approved.



C. H. KRATOCHVIL  
Major, USAF, MC  
Commander

## ABSTRACT

An analog computer was used to compare the dynamic response of an accelerometer placed over the sternum of human test subjects during impact in  $+G_x$  direction with the response of second and higher order spring-mass systems. Identity of the response modes of both systems, human and mechanical, was approximated by trial and error modification of natural frequency and damping coefficient of the computer model used. With restriction to only a few cases investigated and to the particular test conditions, best compliance of complete response coverage is considered to result from the application of a single spring-mass system of irregularly varying damping coefficient. A parametric analysis of the single spring-mass system is presented to aid the use of standardized impact profiles. The usefulness of the method of response approximation has been established, but the validation of the underlying concept of response predictability needs further investigation.

# TABLE OF CONTENTS

	Page
I. INTRODUCTION . . . . .	1
II. THE BIODYNAMIC MODEL . . . . .	3
a. Physical Model . . . . .	4
b. Mathematical Model Modification . . . . .	5
III. EXPERIMENTAL PROCEDURES . . . . .	7
a. Human Testing . . . . .	7
b. Response Approximation . . . . .	9
1. Complete Response Coverage . . . . .	9
2. Limited Response Coverage . . . . .	11
c. Standard Impact Profile (SIP) . . . . .	21
1. Standardization of Impact Profile . . . . .	22
2. Physical Model Response . . . . .	23
IV. ACCURACY OF PROCEDURES . . . . .	23
a. Human Testing . . . . .	23
b. Standardization of Impact Profile . . . . .	27
c. Response Comparison . . . . .	28
V. RESULTS . . . . .	28
VI. RECOMMENDATIONS . . . . .	32
APPENDIX - Analog Computer Response of Second Order Model To Standard Impact Profiles . . . . .	35



# LIST OF TABLES AND ILLUSTRATIONS

	Page
Table I      Selection of Human Tests . . . . .	8
Table II     Accuracy of Recorded Velocity. . . . .	27
Table III    Accuracy of Profile Modification . . . . .	27
Table IV     Comparison of Dynamic Response Data. . . . .	29
Table V      Symbol Chart . . . . .	36
Table VI     Computer Response Data of SIP. . . . .	37
Figure 1     Impact Position. . . . .	3
Figure 2     Physical Spring-Mass System . . . . .	4
Figure 3     Analog Computer Block Diagram . . . . .	6
Figure 4     Complete Response Coverage of Human Test No. 319 . . . .	10
Figure 5     Complete Response Coverage of Human Test No. 612 . . . .	12
Figure 6     Complete Response Coverage of Human Test No. 842 . . . .	13
Figure 7     Limited Response Coverage (First Response Peak) Tests No. 589, 318 and 335 . . . . .	14
Figure 8     Limited Response Coverage (First Response Peak) Tests No. 612, 842 and 319 . . . . .	15
Figure 9     Limited Response Coverage (First Response Peak) Tests No. 607, 755 and 320 . . . . .	16
Figure 10    Limited Response Coverage (First Response Peak) Tests No. 332 and 592 . . . . .	17
Figure 11    Limited Response Coverage (First Response Peak) Tests No. 790 and 606 . . . . .	18
Figure 12    Limited Response Coverage (First Response Peak) Tests No. 751, 798 and 846 . . . . .	19

	Page
Figure 13 Limited Response Coverage (First Response Peak) Tests No. 756 and 844 . . . . .	20
Figure 14 Standard Impact Profile (SIP) . . . . .	21
Figure 15 Impact Profile Standardization . . . . .	22
Figure 16 Amplification Factor Versus Impact Pulse . . . . .	24
Figure 17 Amplification Factor Versus Response Peak Rise Time (Trapezoidal Impact Profiles). . . . .	25
Figure 18 Amplification Factor Versus Response Peak Rise Time (Triangular Impact Profiles) . . . . .	26
Figure 19 Dynamic Characteristic ( $\omega_n$ $\zeta$ ) of Humans Subjected to $+G_x$ Impact . . . . .	31
Figure 20 Continuous Response Modes of SIP (Rectangular Profile). . . . .	43
Figure 21 Continuous Response Modes of SIP (Trapezoidal Profile). . . . .	44
Figure 22 Continuous Response Modes of SIP (Triangular Profile) . . . . .	45

## NOMENCLATURE

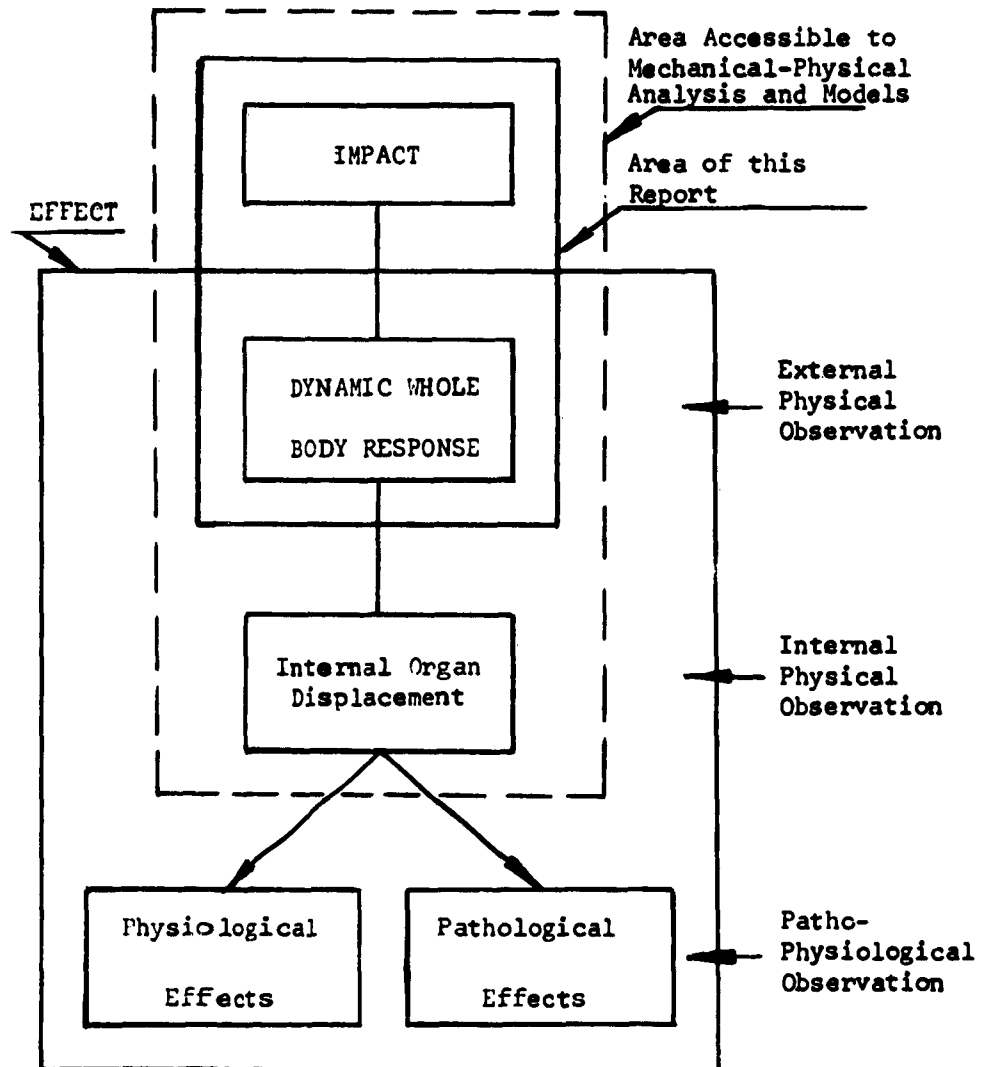
XYZ	Directional components
G	Acceleration factor in multiples of g ft/sec <sup>2</sup>
+G <sub>x</sub>	Acceleration factor in X direction applied to human subjects riding a sled in -X direction, backward facing position
a <sub>i</sub>	Acceleration of sled (accelerometer in terms of +G <sub>x</sub> )
a <sub>i</sub> (t)	Time function of a <sub>i</sub>
a <sub>o</sub>	Acceleration of chest belt (accelerometer) in terms of G
a <sub>o</sub> (t)	Time function of a <sub>o</sub>
$\ddot{x}_i$	Acceleration input into spring-mass model in terms of G
$\ddot{x}_i(t)$	Time function of $\ddot{x}_i$
$\ddot{x}_o$	Acceleration output of spring-mass model in terms of G
$\ddot{x}_o(t)$	Time function of $\ddot{x}_o$
A <sub>i</sub>	Peak acceleration of any impact profile, recorded, approximated or standard
A <sub>o</sub>	First response peak recorded in a <sub>o</sub> (t)
A <sub>o</sub> <sup>*</sup>	First response peak by approximation (feeding the recorded impact function a <sub>i</sub> (t) into the computer model
A <sub>o1</sub> , A <sub>o2</sub> , A <sub>o3</sub>	First, second, third response peak of response function $\ddot{x}_o(t)$ of Standard Impact Profile A <sub>i</sub> (σ <sub>1</sub> , σ <sub>2</sub> , τ)
t <sub>A<sub>o</sub></sub> , t <sub>A<sub>o</sub></sub> <sup>*</sup> , t <sub>A<sub>o1</sub></sub>	Respective rise times of A <sub>o</sub> , A <sub>o</sub> <sup>*</sup> , A <sub>o1</sub>
A <sub>i</sub> (σ <sub>1</sub> , σ <sub>2</sub> , τ)	Standard Impact Profile (SIP), geometrically standardized shape of impact
τ	Total impact duration time of SIP
σ <sub>1</sub>	Time factor in terms of τ of onset time of impact peak acceleration A <sub>i</sub> of SIP
σ <sub>2</sub> - σ <sub>1</sub>	Duration time of impact peak acceleration A <sub>i</sub> in terms of τ

$\omega_n$	Undamped natural frequency ( $\sqrt{k/m}$ ) of SIP
$\omega_n^*$	Undamped, natural frequency of human chest
$T = \frac{2\pi}{\omega}$	Response established by trial and error approximation
$\zeta$	Damping factor of SIP
$\zeta^*$	Damping factor of human chest response established by trial and error approximation
$\zeta_i^*$	Initial value of $\zeta^*$ before changes

# I

## INTRODUCTION

One reason for analyzing the effects of impact on man through treatment of the body as a dynamic mechanical system is founded in the hope of developing models which permit extrapolation from known test exposures of human subjects to injury criteria for untested acceleration environments. The overall approach underlying the development of such models is illustrated by the following diagram of the schematic breakdown of biodynamic response to impact.



As shown, the impact environment acts on critical internal body structures to produce forces, organ displacements and deformations whose peak value and variation with time are a function of the dynamic response characteristics of the body in general, and of the particular structure and substructure, in particular. Any physiological or behavioral response to, or any pathological manifestation of impact is directly related to this dynamic response of the body or, more precisely, a result of relative displacement of one tissue structure with respect to another. The strain may produce either a disruption of structure resulting in frank injury or, short of mechanical fatigue or injury, the strain may induce alterations in the control mechanisms of the body which are manifest as changes in physiological parameters. The quantitation of pathophysiologic changes produced by high magnitude impacts usually requires examination of the specimen in detail and analysis of monitored physiologic data, which is not possible except in animal experiments. Cineradiographic techniques which are currently being refined are providing the possibility to begin studying the motions of internal organs, which will permit further quantitation of the dynamic response characteristics of segments of the body to impact.

Only through such detailed quantitative studies of the transmission of the mechanical energy from the environment to the point inside the body of final biological effectiveness, can one hope to achieve a more detailed quantitative understanding of the body's biological response as is presently available.

This paper deals with the first step in this direction by analyzing dynamic whole body response to impact. The data were obtained in connection with a large series of human tolerance tests on the Daisy Decelerator and were originally not primarily collected for this purpose. The dynamic response analyzed is the acceleration of the surface overlying the sternum of a seated subject exposed to  $+G_x$  impact.

The method of analysis for the correlations between response and impact is in terms of the development of parameters for a spring-mass system with a similar excitation and response. The correlations are to be developed in terms of the characteristics of the impact such as peak value, onset rate, duration and offset rate and in terms of the characteristics of the equivalent spring-mass system such as resonant frequency and damping factor and variations of these parameters.

## II

### THE BIODYNAMIC MODEL

The usefulness of the chosen biodynamic model is restricted to those body components directly or indirectly effected by or effective in the dynamic response of the thorax. Additional limitation accrues from the necessity due to the complex arrangements and properties of these body components to apply a model of analogy with reference to the involved body components as a lumped system rather than a model of true simulation.

The experimental conditions, described later, are illustrated by Figure 1.

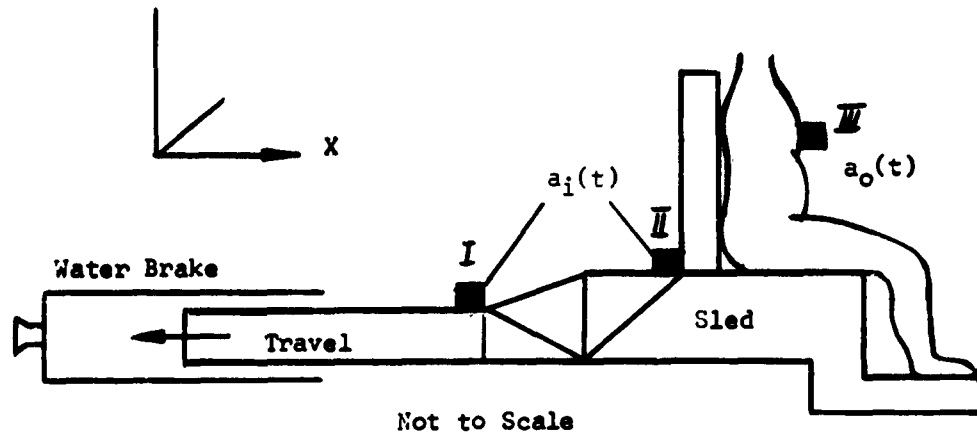


Figure 1 Impact Position

The human subject, seated on a sled, entered the water brake of the Daisy Decelerator in backward riding position (+G<sub>x</sub>). The impact pulse  $a_i(t)$  in X direction was measured by accelerometers placed on the piston (I) or the sled structure (II) behind the seat. The dynamic response  $a_o(t)$  of the subject's chest was measured by accelerometers placed over the sternum (III) of the test subject clothed in a single layer surgical suit. The coordinates of measurements at location III (chest) are fixed with the accelerometer pad mounted on a chest belt applied over the suit. The sled/body mass ratio was about 10:1.

a. Physical Model (Figure 2)

Since accelerometer measurements always refer to the earthbound coordinate system it was desired that the chosen derivation of the differential equation concurs with the applied instrumentation.

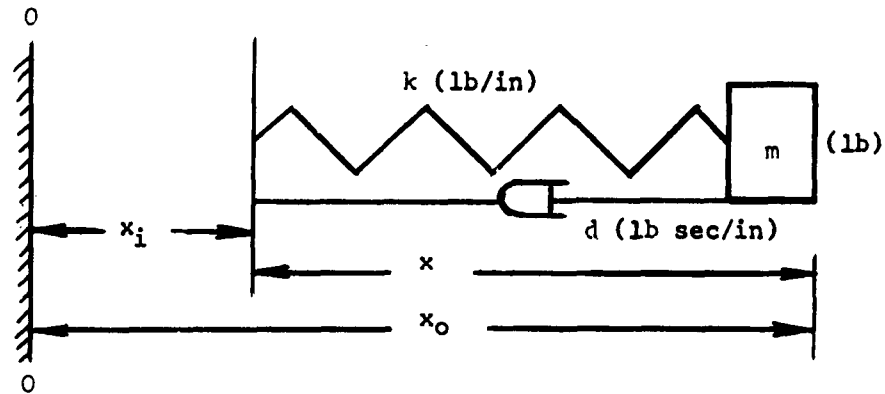


Figure 2 Physical Spring-Mass System

With line 0-0 as earth fixed reference, the differential equation of the assumed spring-mass system is written in the form:

$$\ddot{x}_o + \frac{d}{m} \dot{x} = \frac{k}{m} x = 0 \quad (1)$$

$\ddot{x}_o$  is the acceleration of the assumed mass  $m$  to be compared with the (output) measurement  $a_o$  of the chest accelerometer at location III (Fig. 1). The displacement  $x_o$  of the mass  $m$  is thought to be not identical with the elongation  $x$  of the assumed spring. Since the spring mass system is used as a model of analogy, the mass  $m$  (lb),



the damping factor  $d$  (lb sec/in), and the spring constant  $k$  (lb/in) of this physical model do not have any known relation to the physical properties of the body (components). It is the purpose of this study to investigate whether or not the dynamic response characteristics of the human trunk exposed to  $+G_x$  impact can be simulated by a simple spring-mass system in terms of undamped natural frequency  $\omega_n (= \sqrt{k/m})$  and dimensionless damping coefficient  $\zeta (= 1/2 d / \sqrt{mk})$ .

By use of

$$x = x_o - x_i ; \dot{x} = \dot{x}_o - \dot{x}_i$$

and the substitutes

$$k/m = \omega_n^2 \text{ and } d/m = 2\zeta\omega_n$$

equation (1) is transformed into

$$\ddot{x}_o + 2\zeta\omega_n\dot{x}_o + \omega_n^2 x_o = 2\zeta\omega_n\dot{x}_i + \omega_n^2 x_i \quad (2)$$

In Laplace notation, equation (2) can be written as the transfer function

$$\frac{x_o(s)}{x_i(s)} = \frac{2\zeta\omega_n s + \omega_n^2}{s^2 + 2\zeta\omega_n s + \omega_n^2} \quad (3)$$

where  $s$  is the commonly used Laplace Operator.

Multiply both sides of the equation with  $s^2$  it is

$$\frac{x_o(s)s^2}{x_i(s)s^2} = \frac{\ddot{x}_o}{\ddot{x}_i}$$

Where  $\ddot{x}_i$  and  $\ddot{x}_o$  can be compared with the acceleration  $a_i$  and  $a_o$  measured at location I (or II) and III respectively (Fig. 1).

On the analog computer, equation (3) was mechanized with  $\omega_n$  and  $\zeta$  as adjustable variables (Fig. 3). A time expansion of 100 was used for convenience.

#### b. Mathematical Model Modification

The second order system (equation 3) can be enlarged to the fourth or sixth order by writing

$$\frac{a_1 s + b_1}{(s^2 + a_1 s + b_1)(s^2 + a_2 s + b_2)}$$



respectively

$$\frac{a_1 s + b_1}{(s^2 + a_1 s + b_1)(s^2 + a_2 s + b_2)(s^2 + a_3 s + b_3)}$$

identified by the factors

$$\omega_{n1}, \omega_{n2}, \omega_{n3}, \zeta_1, \zeta_2, \text{ and } \zeta_3.$$

This modification cannot be identified with a set of coupled spring-mass systems unless one would neglect the reaction of the second system to the first and so forth. However, the mathematical model modification can be used for qualitative comparison between second order and higher order systems.

### III

#### EXPERIMENTAL PROCEDURES

##### a. Human Testing

The human impact tests under consideration were not designed to satisfy the technical aspects of this study but were governed by the objectives of typical go-no-go testing; i.e., in each case the test subject was observed by physical examination as to his hematological responses as the reaction to a particular impact pulse applied to the test sled.

In application to this study, it was hoped that test subjects having had more than one run might offer a better chance of a recognition of trends. On this basis only the tests of Table I were selected from available series of backward-facing (+G<sub>x</sub>) impact.

The tests used comprise a number of instrumentational changes. No recordings of physiological data were made prior to test No. 359. Only the acceleration-time histories of the sled,  $a_1(t)$ , and of the human chest  $a_0(t)$ , were recorded. Two accelerometers, both measuring in X direction were mounted on the sled piston (location I). Two accelerometers placed over the sternum (location III) of the test subject also were oriented in X direction; however, tilting of the chest accelerometers, i.e., the position of their coordinates, was not controlled during impact.

Table I Selection of Human Tests

Test No.	Test No.	Subject Name	Height (in)	Weight (lbs)	Sled (A <sub>i</sub> ) Peak "G"	Chest (A <sub>o</sub> ) Peak "G"	Test Variation
318	I	ELB	70	135	25/26	66/43	The "# 300" series measurements are less reliable than all other subsequent tests for which a more stable accelerometer mounting was used.
335				135	40	86/78	
589				140	14	21.5	
319	II	JDM	70	155	25.5	38	
612				171	15	23.5	
842				169	20	31	
320	III	RAG	69	170	23.5	43	
607				175	14	25	
755				172	20.5	29.5	
332	IV	AVZ	65	118	36.5	54	
592				120	15	22	
606	V	RH	67	150	16	27.5	*
790				155	10.5	18	
751	VI	MCS	68	155	19	22	*
846				160	19	33	
798				154	23.5	27	
756	VII	CHSW	67	145	21.5	27.5	
844				150	20	29	

\* In these tests a 24-pound parachute (including harness) was placed over the chest of the test subject and the response accelerometer was placed over the chest parachute.

With test No. 359, a change of the chest and sled instrumentation was introduced. At both locations I and III, three accelerometers, recording in three coordinates X, Y, and Z, were applied. Only the recordings in X direction were used in this analysis. A double chest strap was used to accommodate the chest accelerometers, with coordinate positions still uncontrolled during impact. Test No. 390 and all consecutive tests included ECG recording. Starting with test No. 592, the three sled accelerometers were removed from the sled piston (location I) and mounted at the sled structure closer to the seat (location II).

Tests No. 300 through 335 are reported in a previous publication<sup>1</sup>.

#### b. Response Approximation

The records of the impact acceleration  $a_i(t)$  measured at location I (or II) were used as the input function  $\ddot{x}_i(t)$  of the computer and were transformed by a curve follower into volts as a function of time. The output function  $\ddot{x}_o(t)$  of the computer was plotted by an x-y plotter on translucent paper overlaying the pre-drawn, actually recorded chest acceleration  $a_o(t)$  measured at the sternum of the test subject (location III). Potentiometers for  $\omega_n^*$  and  $\zeta^*$  were controlled manually in successive computer runs until a close fit between computer output  $\ddot{x}_o(t)$  and recorded chest response  $a_o(t)$  was achieved.

##### 1. Complete Response Coverage

The physical model second order (Section IIa) and its mathematical modification to a model of higher order up to the sixth (Section IIb) were used to determine the significance of the choice variables. Tests No. 319, 612 and 842 are discussed as typical examples:

Test No. 319 (Fig. 4). A second-order system of constant  $\omega_n^* = 163$  rad/sec and constant damping coefficient  $\zeta^* = 0.65$  failed to approach the acceleration-time history of the record. By use of two second-order systems ( $\omega_{n1}^* = 163$ ,  $\omega_{n2}^* = 194$ ) satisfactory compliance of the complete response mode could be obtained but only with the damping coefficient  $\zeta_2^*$  varying from 0.03 to 0.9 after a time of 0.0625 second, with a constant setting of  $\zeta_1^* = 0.65$ .

---

<sup>1</sup> Beeding, Eli L., and John D. Mosely. Human Deceleration Tests. AFMDC-TN-60-2, Holloman AFB, New Mexico, January 1960.

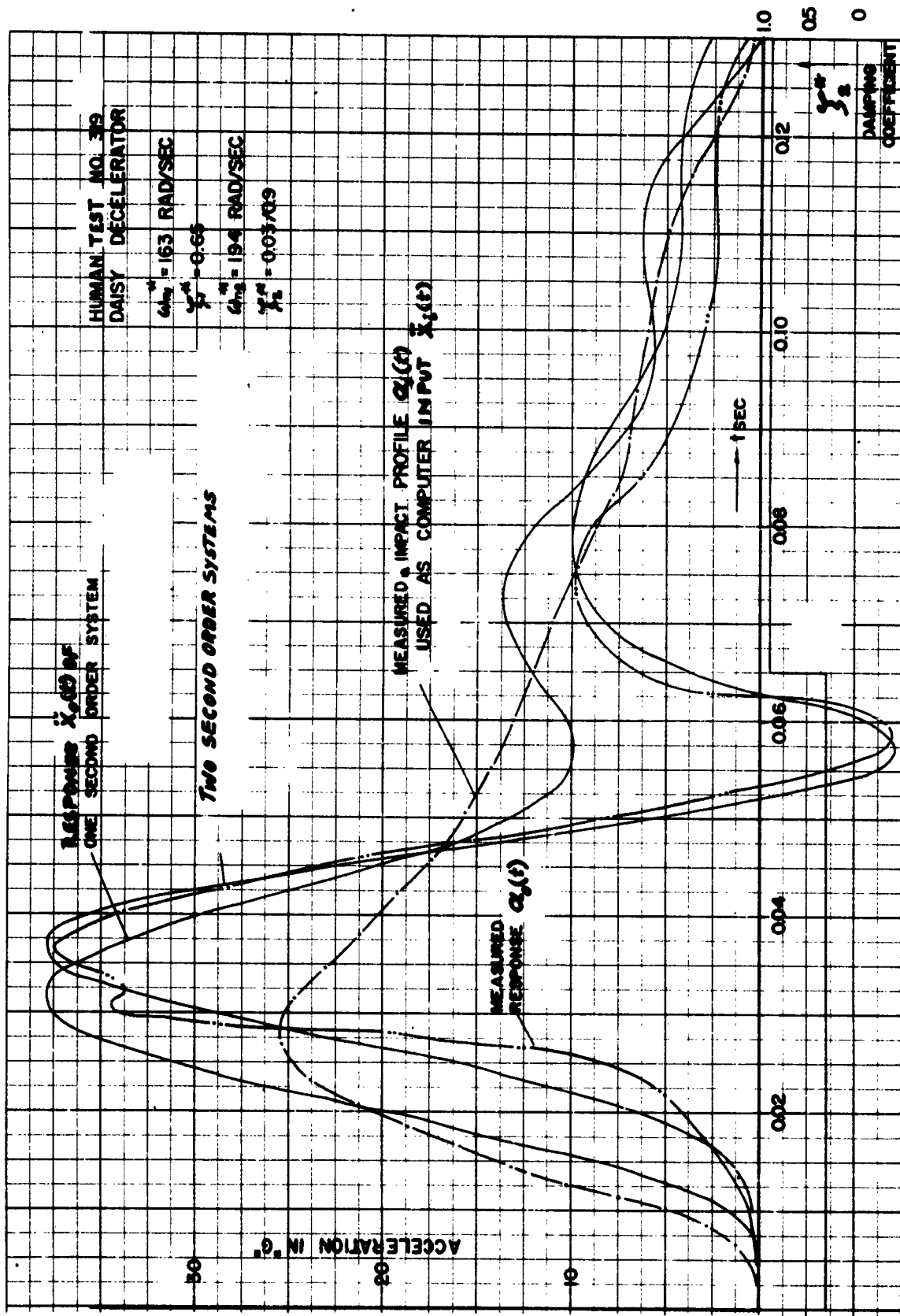


Figure 4 Complete Response Coverage of Human Test No. 319

Test No. 612 (Fig. 5). Compliance was considered satisfactory for constant  $\omega_n^* = 145$  rad/sec and a change of the damping coefficient from 0.25 to 0.75 at the time of 0.045 second.

Test No. 842 (Fig. 6). Comparison is made for a second-order system between two approaches, one of constant  $\omega_n^*$  and constant  $\zeta^*$ , the other of constant  $\zeta^*$  and continuously varying  $\omega_n^*$ . In this test, response peak and onset time were approximated somewhat better by varying  $\omega_n^*$ .

## 2. Limited Response Coverage

All tests were rerun on the computer with the requirement to establish best compliance of first response peak and its onset time by use of the second order, physical model (Section IIa) for constant  $\omega_n^*$  (per run) and constant damping coefficient  $\zeta^*$  (per run). The results are illustrated in Figures 7 through 13. Natural frequency  $\omega_n^*$  and damping  $\zeta^*$  are considered as criteria of comparison between runs of same and different test subjects.

Test No. 318 and 335, Figure 7, illustrate a very erratic onset of the input peaks of 26G and 40G respectively, recorded at location I of the sled (Fig. 1). Test No. 319, Figure 8, shows a very unrealistic double peak of the dynamic chest response  $a_o(t)$ . For both tests the highest response peak  $A_o$  recorded by accelerometer No. a of 66G and 86G could not be simulated by the computer for any value of  $\omega_n^*$ . The differences of response peaks of same test No. 318 recorded by accelerometers Nos. a and b could not be explained as to their cause. Therefore, the response data of the "No. 300" test series cannot be used for comparison.

Tests No. 790 and 798, Figures 11 and 12 respectively, differ from all other tests by the use of a 24-pound chest parachute to which the accelerometer pad was attached for otherwise unchanged test conditions. Here, too, a comparison with other tests might be misleading.

All other plottings of Figures 7 through 13 are self-explanatory. In each case the electronic recording system filtered out all vibration frequencies beyond 300 c.p.s. of the sled impact pulse measured at location I or II. The recording of the chest response dynamics (location III) was usually not superimposed by noise.

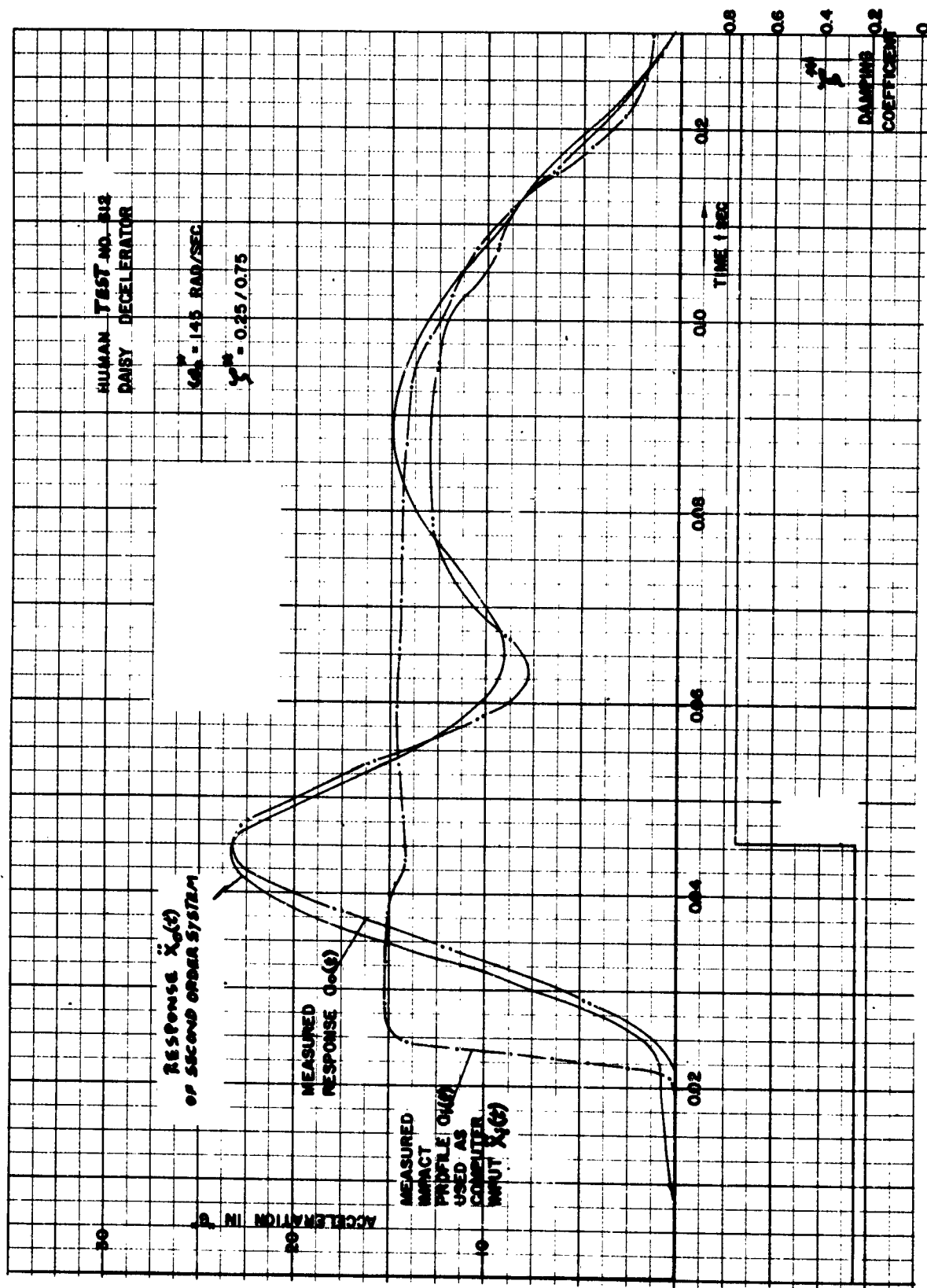


Figure 5 Complete Response Coverage of Human Test No. 612



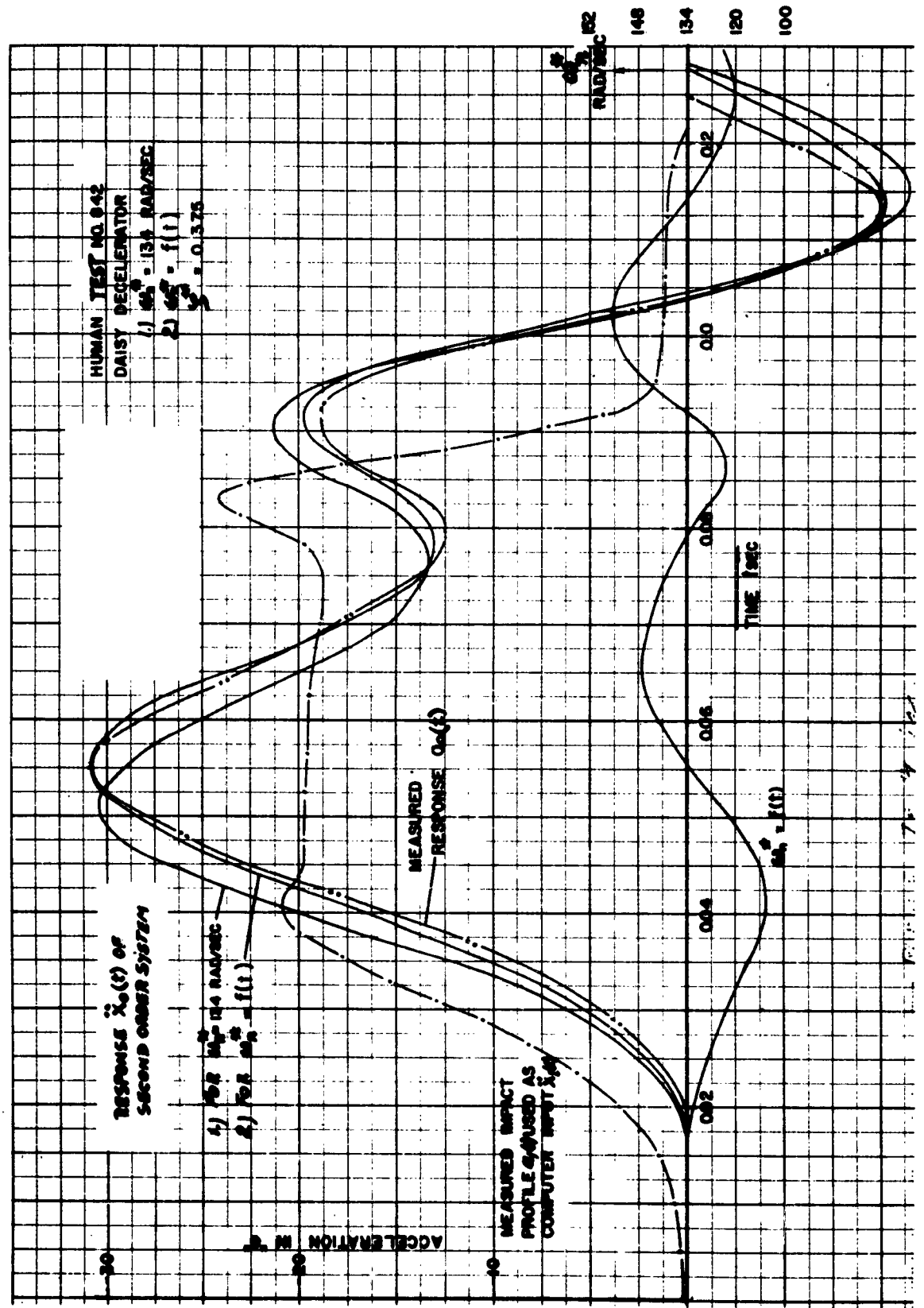


Figure 6 Complete Response Coverage of Human Test No. 842

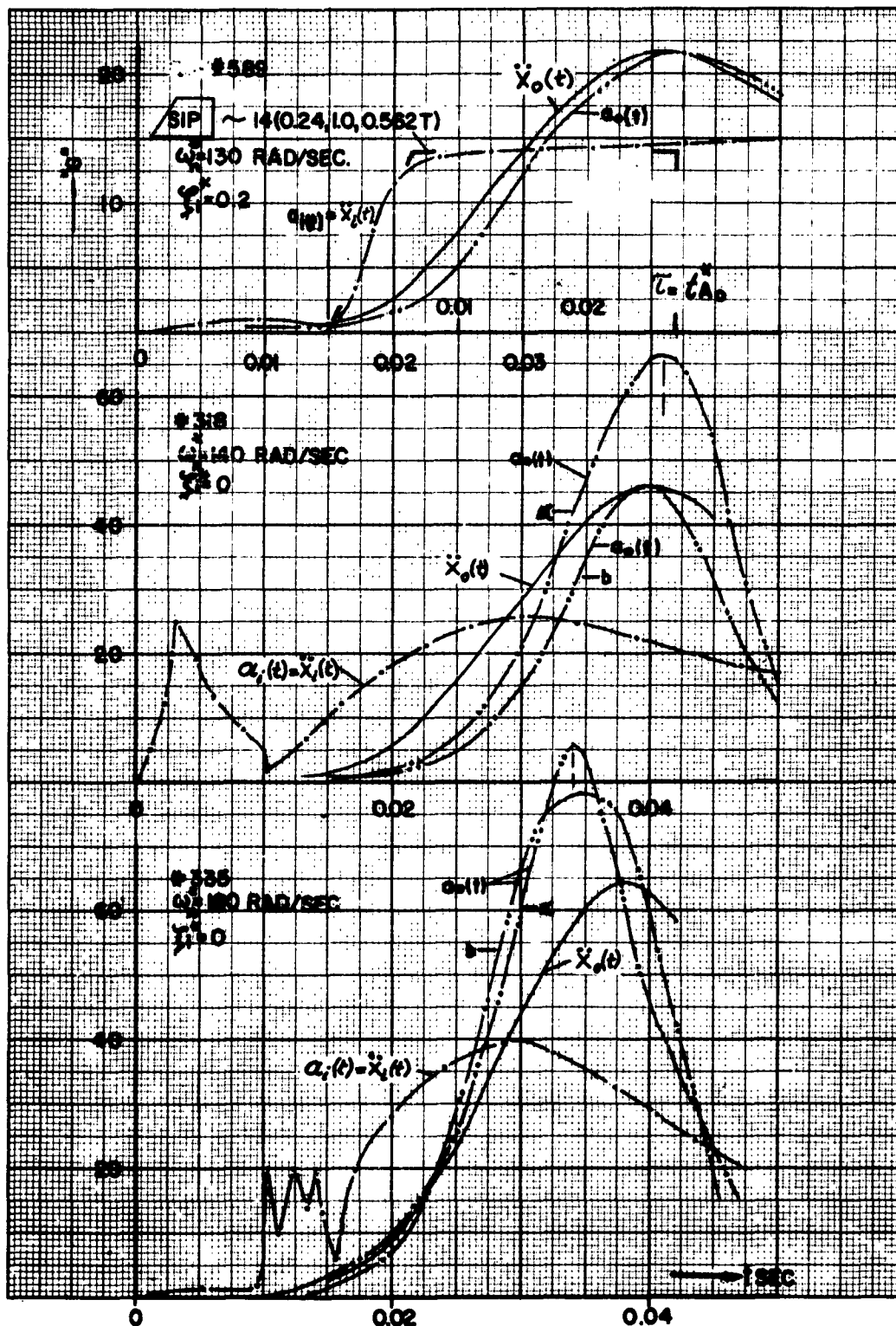


Figure 7 Limited Response Coverage (First Response Peak)  
Tests No. 589, 318 and 335.

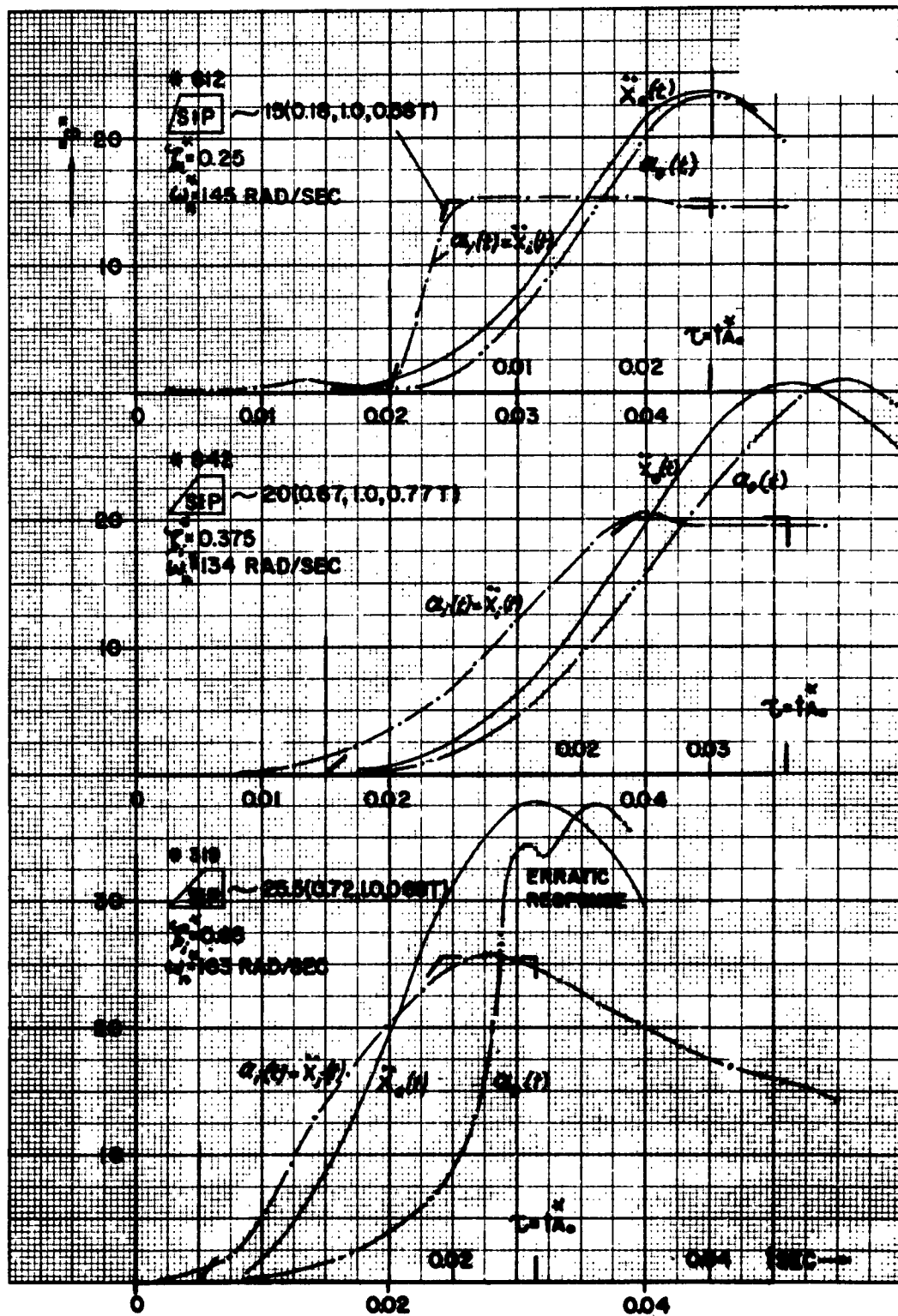


Figure 8 Limited Response Coverage (First Response Peak)  
Tests No. 612, 842 and 319.

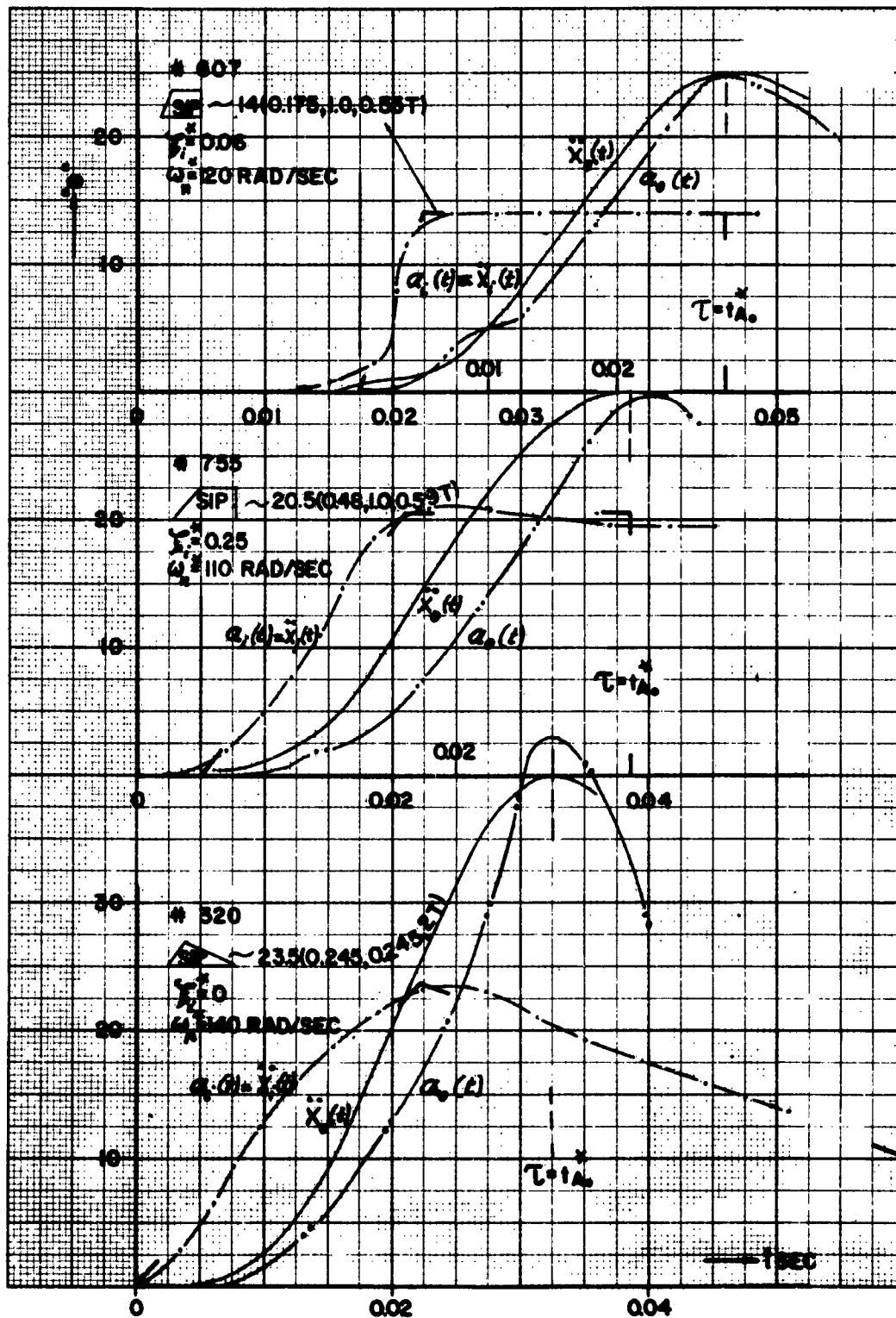


Figure 9 Limited Response Coverage (First Response Peak)  
Tests No. 607, 755 and 320.

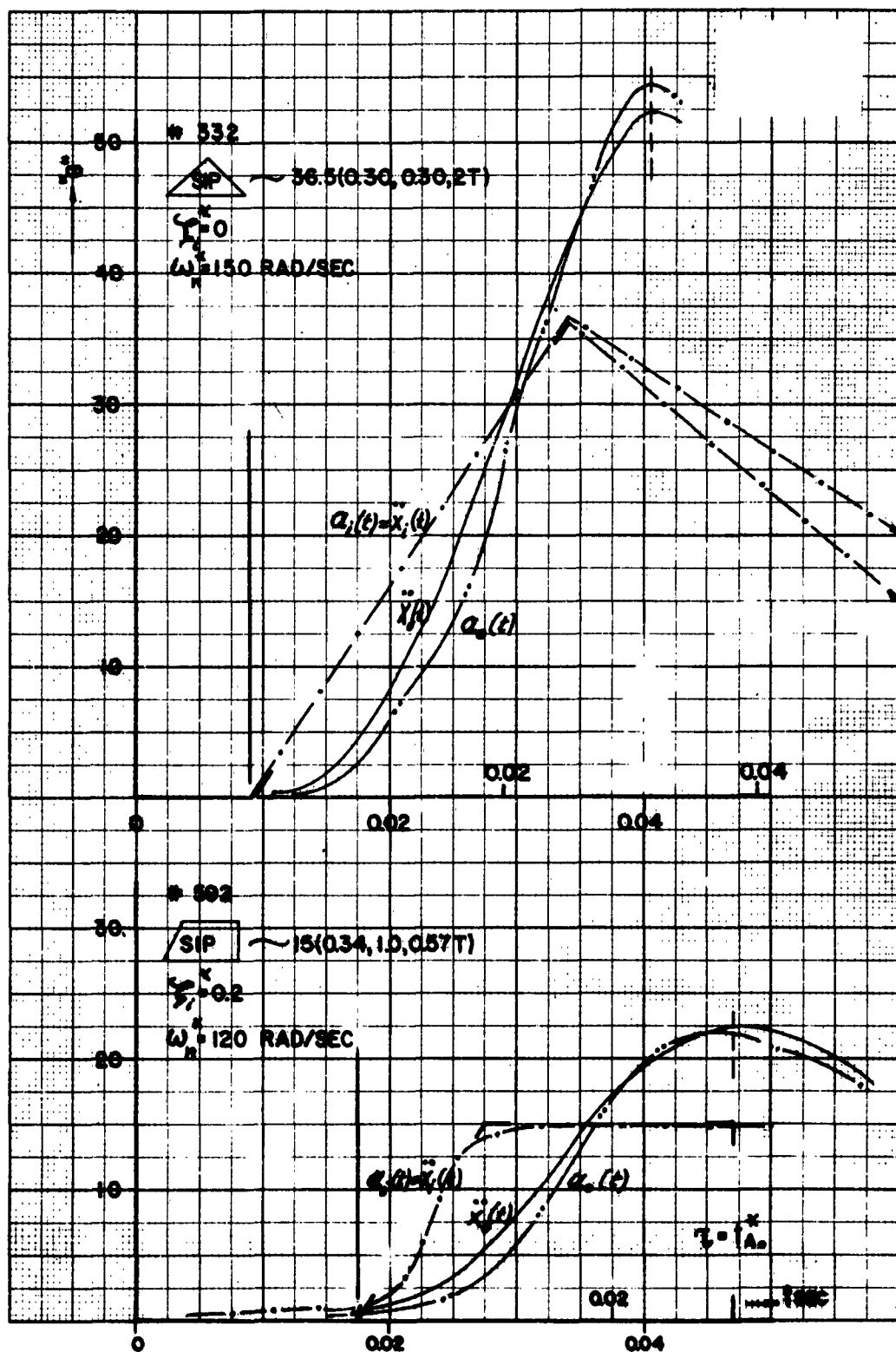


Figure 10 Limited Response Coverage (First Response Peak)  
 Tests No. 332 and 592.

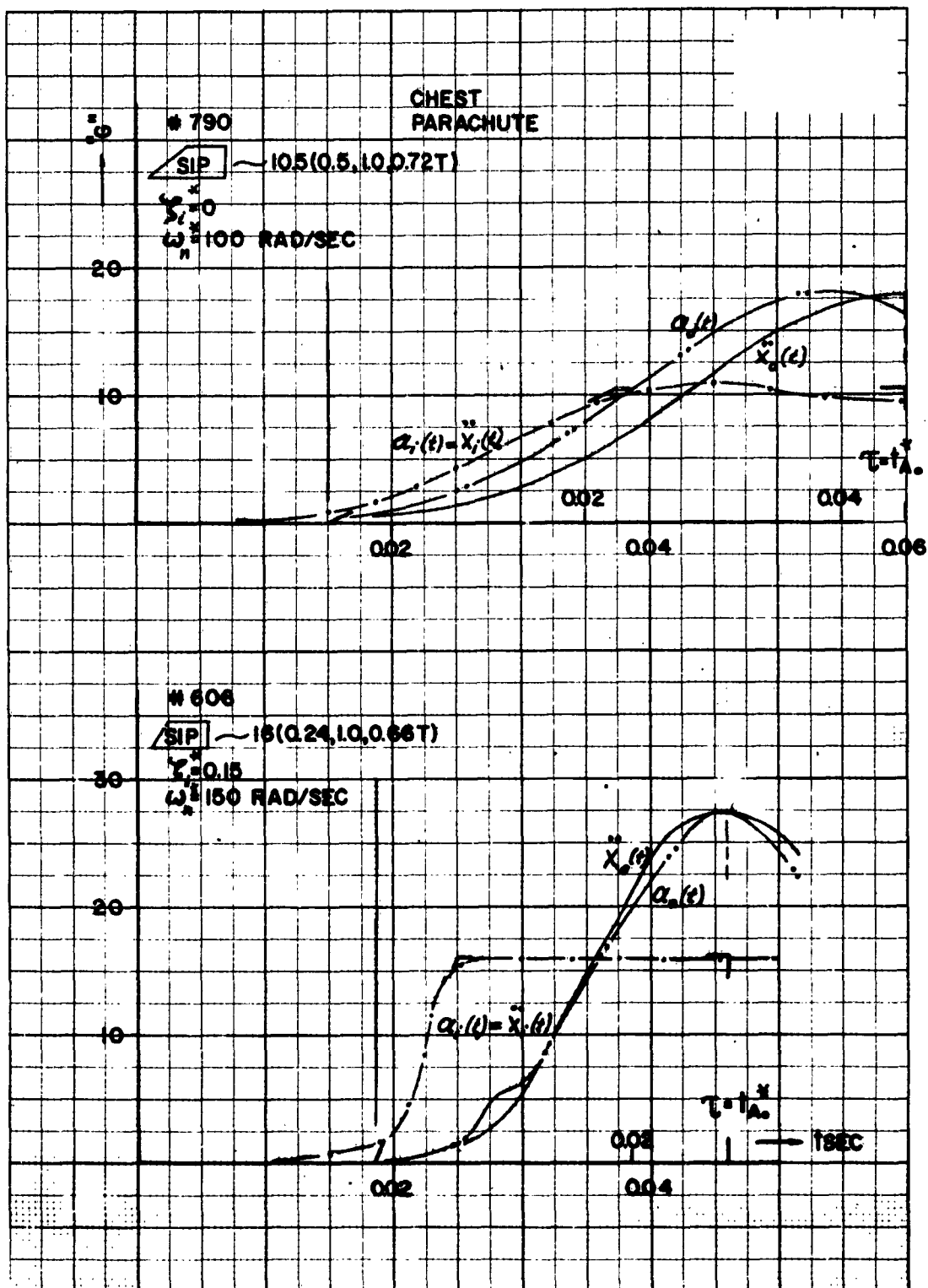


Figure 11 Limited Response Coverage (First Response Peak)  
Tests No. 790 and 606.

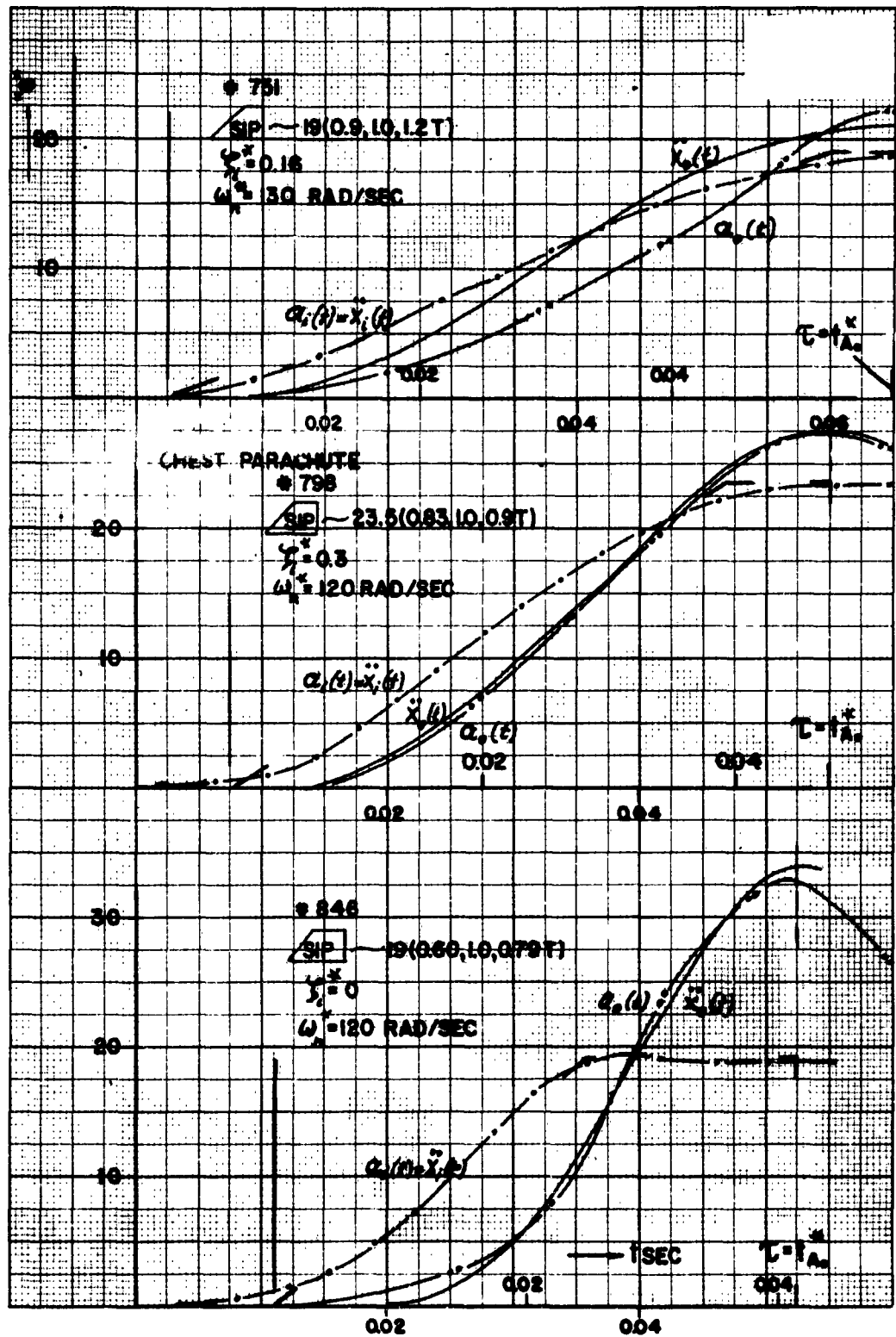


Figure 12 Limited Response Coverage (First Response Peak)  
Tests No. 751, 798 and 846.

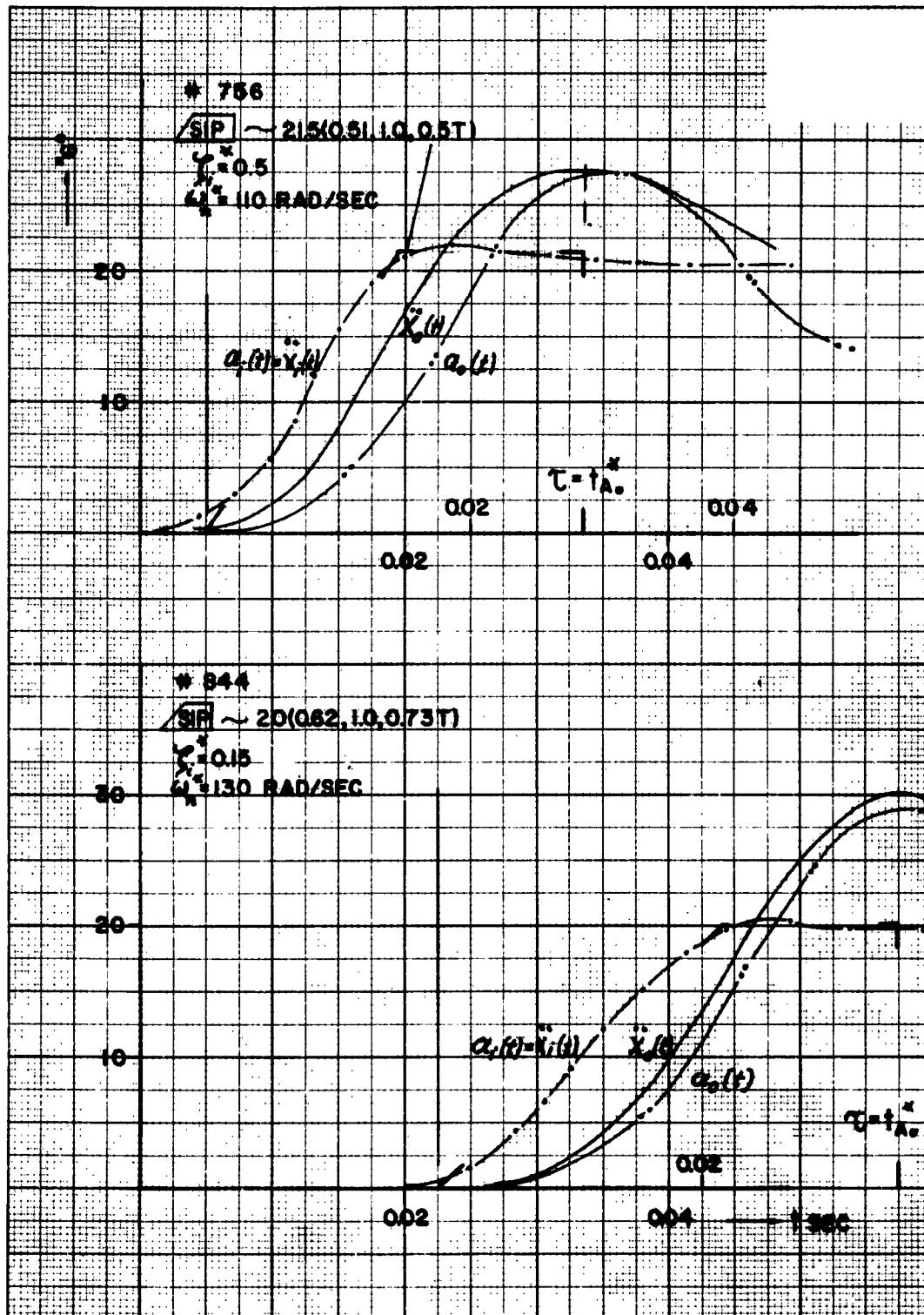


Figure 13 Limited Response Coverage (First Response Peak)  
 Tests No. 756 and 844.



The recorded impact profiles  $a_i(t)$  as measured at sled locations I or II were "hand smoothed" (Section IVb) before being applied as the input profile  $\ddot{x}_i(t)$  of the computer model. In addition, the "hand smoothed" impact profiles were replaced by standardized impact profiles in an attempt to generalize the test evaluation as outlined in the following section.

c. Standard Impact Profile (SIP)

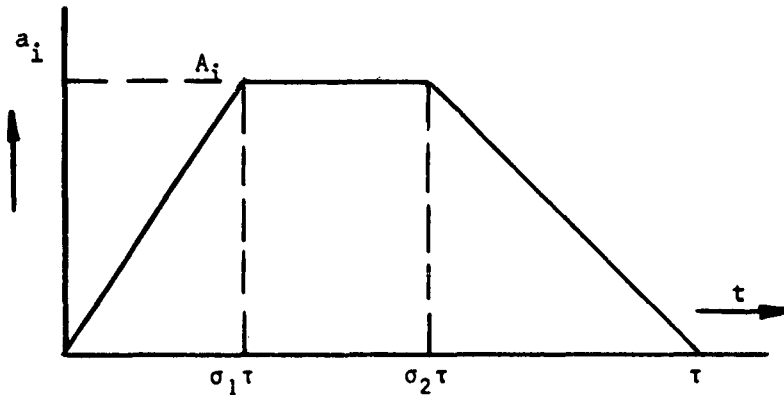


Figure 14 Standard Impact Profile

The Standard Impact Profile (SIP) can be termed symbolically as  $SIP \sim A_i(\sigma_1, \sigma_2, \tau)$  where  $A_i$  is the peak acceleration,  $\tau$  the impact duration,  $\sigma_1$  the time factor of peak onset, and  $\sigma_2 - \sigma_1$  the time factor of peak duration with reference to  $\tau$ .

The impact parameters for this profile are given in explicit form<sup>2</sup> for accelerated motion,

$$D = \frac{\sigma_1^2 - \sigma_2^2 - 3\sigma_1 + 2\sigma_2 + 2}{3(1 + \sigma_2 - \sigma_1)} \cdot v_f \tau \quad ; \quad A_i = \frac{2}{1 + \sigma_2 - \sigma_1} \cdot \frac{v_f}{\tau}$$

---

<sup>2</sup> Feder, H.C. Nomographs for Multiphase Acceleration Profiles. AFMDC-TR-60-9, Holloman AFB, New Mexico, June 1960.

for decelerated motion,

$$D = \frac{\sigma_2^2 - \sigma_1^2 + \sigma_2 + 1}{3(1 + \sigma_2 - \sigma_1)} \cdot v_i \tau ; A_i = \frac{2}{1 + \sigma_2 - \sigma_1} \cdot \frac{v_i}{\tau}$$

(D = travel distance,  $v_f$  = final velocity of acceleration, initial velocity zero,  $v_i$  = initial velocity of deceleration, final velocity zero.) These equations are useful for test programming and evaluation in regard to  $A_i$ , D, v, and  $\tau$  for variable values of  $\sigma_1$  and  $\sigma_2$ .

### 1. Standardization of Impact Profile

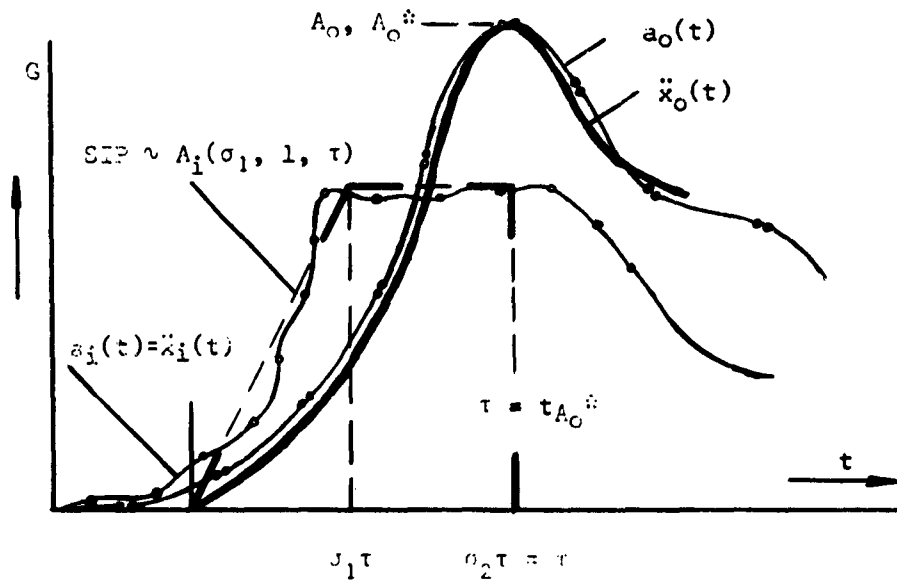


Figure 15 Impact Profile Standardization

Most impact recordings are of irregular shape and not shown in the report. The "hand smoothed" impact profiles  $a_i(t)$  in Figures 7 through 13 have been standardized as explained by Figure 15. The standardization is achieved by replacing the initial part of the recorded, but "hand smoothed" impact profile  $a_i(t)$  by a standard impact profile  $A_i(\sigma_1, \sigma_2, \tau)$ . Only those replacements for  $\sigma_2 = 1$  are described in this report. (In all other cases,  $\sigma_2 \neq 1$ , similar procedures can be applied.) The total impact pulse time  $\tau$  of the

replacing standard impact profile  $A_i(\sigma_1, 1, \tau)$  is identified by the time  $t_{A_0}^*$  at which the response peak  $A_0^*$  resulting from the trial and error computer approximation  $\ddot{x}_0(t) \rightarrow a_0(t)$  by use of the "hand smoothed" impact (input) profile  $a_i(t) = \ddot{x}_i(t)$  is found.

The impact peak level  $A_i$  is the same for all profiles, original  $a_i(t)$  or standardized  $A_i(\sigma_1, 1, \tau)$ .

## 2. Physical Model Response (Appendix)

The computer data of the second-order spring-mass system (Section IIa) excited by standard impact profiles have been plotted in Figures 16, 17 and 18. Response peak level and rise time are represented by the symbols  $A$  and  $t_A$  with the subscripts  $i, o1, o2, o3$ , identifying input, output, first, second, and third peak respectively.

Figure 16, restricted to  $\zeta = 0$ , illustrates that clear dependencies exist for impact durations up to  $\tau = T/2$ . In the range  $\tau = T/2$  to  $2T$  the applied plotting of only three points proves to be insufficient for use of interpolation. Additional measurements would be necessary to clarify this area.

Figures 17 and 18 apply a particular plotting insofar as the rise time  $t_{A_{o1}}$  of the response peak  $A_{o1}$  is used as a reference parameter.

## IV

### ACCURACY OF PROCEDURES

#### a. Human Testing

A comparison between the sled entrance velocity and the measured impact history  $v_{(\text{entrance})} \sim \int a_i dt_{(\text{impact})}$  is the only means of relative accuracy survey since no direct accuracy controls of velocity or acceleration were available. The entrance velocity was measured by use of break wires (Berkley counters); the integration of the complete acceleration-time tracks of the original records (as far as available) was achieved by use of a planimeter, including all shock type oscillations inherent in these recordings. The data are given in Table II.

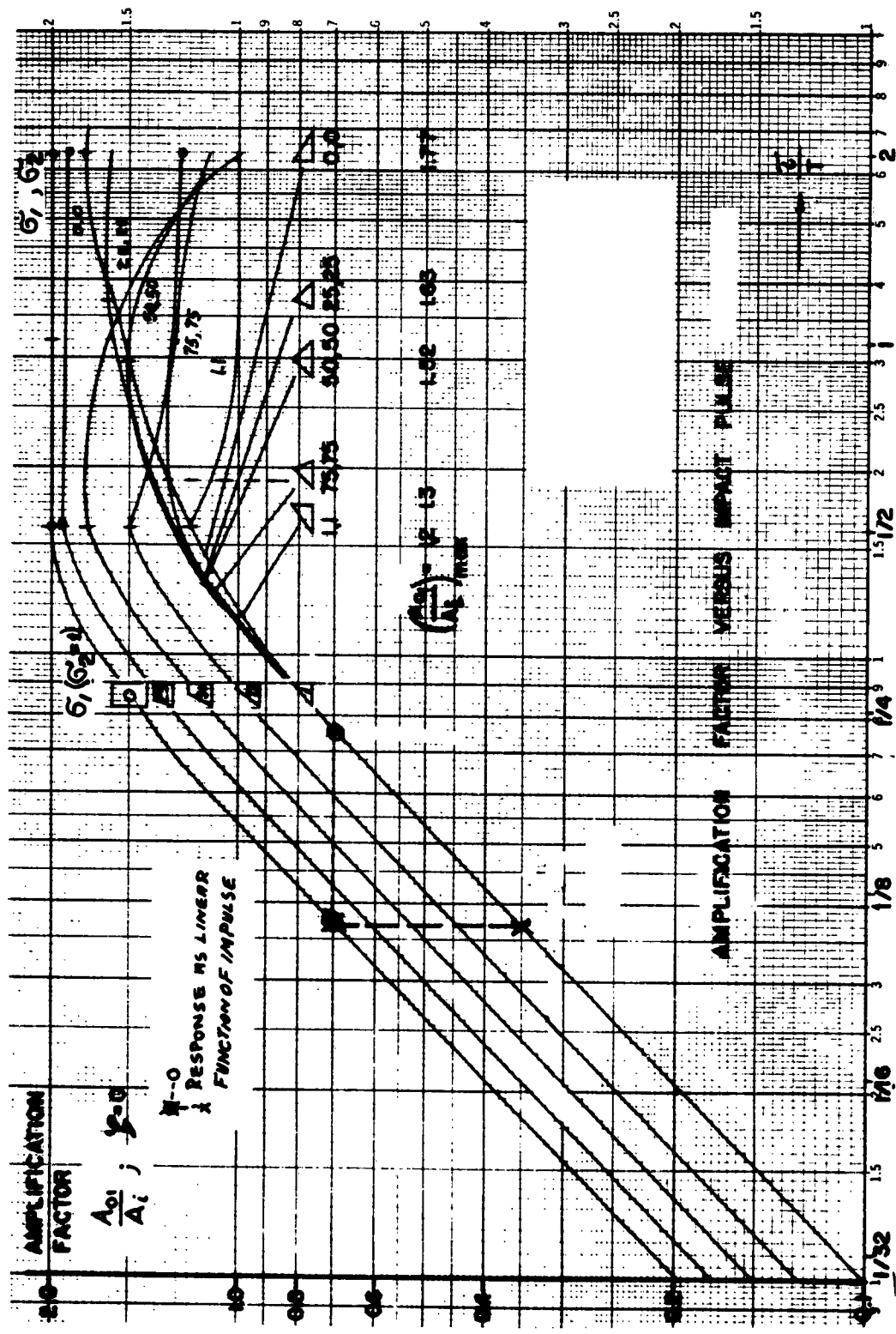


Figure 16 Amplification Factor Versus Impact Pulse

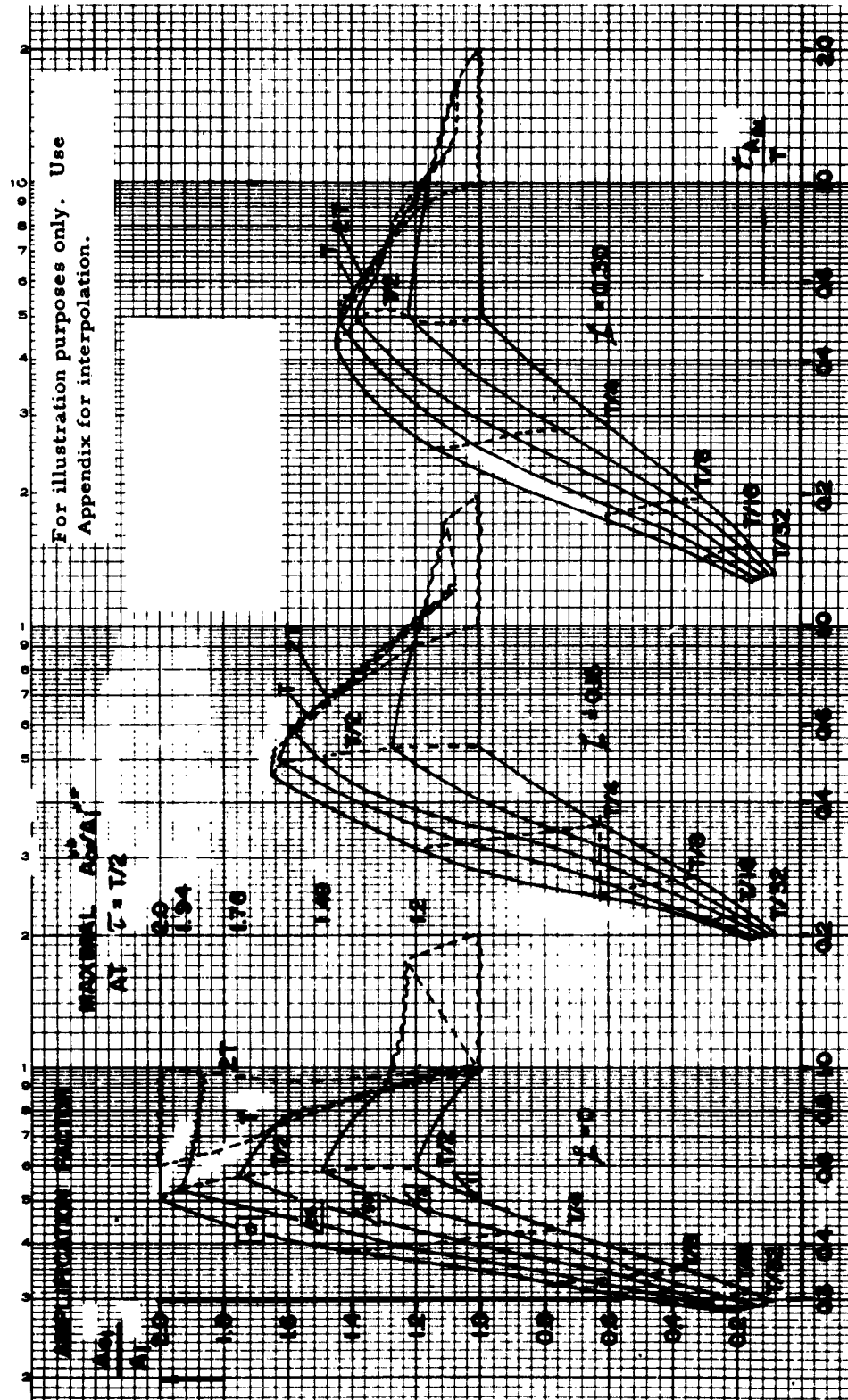


Figure 17 Amplification Factor Versus Response Peak Rise Time  
(Trapezoidal Impact Profiles)

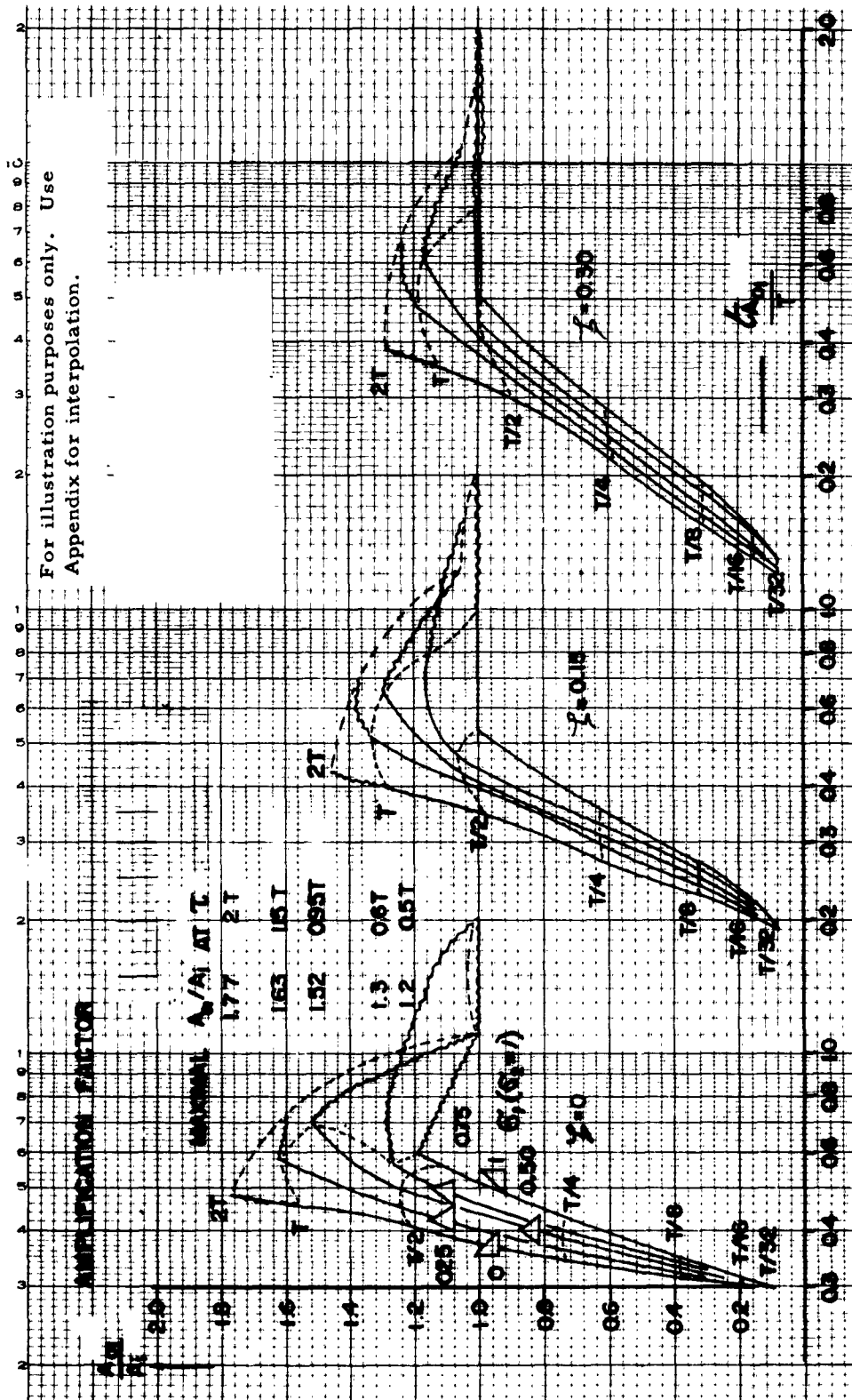


Table II Accuracy of Recordings

<u>Test No.</u>	<u>Entrance Velocity ft/sec</u>	
	<u>v</u> <u>(Breakwire)</u>	<u><math>\int a_i dt</math></u> <u>(Planimeter)</u>
335	48.1	44.6
319	47.4	42.5
612	44.4	40.0
842	40.3	41.6
790	40.4	39.7
846	39.7	40.0
798	49.2	47.0
756	57.8	65.5
847	43.6	42.8

b. Standardization of Impact Profile

Both "hand smoothing" of the original tracks and standardization  $A_i(\sigma_1, l, \tau)$  of the "hand smoothed" profiles  $a_i(t)$  presented in this report were achieved manually. This manipulation can be only vaguely described as a procedure of averaging at the discretion of the evaluator. With reference to the rise time  $t_{A_{01}}$  of the first response peak  $A_{01}$  resulting from the standard profile  $A_i(\sigma_1, l, \tau)$ , the original tracks, the "hand smoothed" profiles  $a_i(t)$  and the standardized profiles  $A_i(\sigma_1, l, \tau)$  were integrated by use of a planimeter and are reported in Table III.

Table III Accuracy of Profile Modification

<u>Test No.</u>	<u><math>\int a_i dt</math> (ft/sec)</u>		
	<u>Original track</u>	<u>Hand smoothed profile <math>a_i(t)</math></u>	<u>Standardized profile <math>A_i(\sigma_1, l, \tau)</math></u>
319	15.9	13.6	13.6
335	27.4	21.5	---
612	9.3	11.5	11.0
756	13.8	14.1	14.6
790	11.5	11.9	12.5
798	19.1	19.5	20.4
842	26.1	15.5	15.3
844	15.1	15.5	15.1
846	16.5	17.4	17.8

### c. Response Comparison

A comparison of the response peak levels and their rise times of the test records ( $A_o$ ,  $t_{A_o}$ ) and of the spring-mass model applied with the recorded impact profile  $a_i(t)$  by use of trial and error approximation ( $A_o^*$ ,  $t_{A_o}^*$ ) and with the standard impact profile ( $A_{o1}$ ,  $t_{A_{o1}}$ ) is given in Table IV.

Whenever  $A_{o1}/A_i$  could be found by interpolation of Figures 17 and 18, this amplification factor was used to determine the response peak  $A_{o1}$ . Otherwise, the factor  $A_{o1}/A_i$  was computed by use of  $A_o^*/A_i$ . Similarly, the response peak rise time  $t_{A_{o1}}$  was found by interpolation or by use of  $t_{A_o}^*/T$ .

Of course, the experimental data from Figures 7 through 13 with reference to the standardized profile are identical with the data gained from the physical model based on standard impact profiles of Figures 17 and 18 if identical values of  $\omega_n$  and  $\zeta_i$  are applied. Consequently, a comparison between the recorded and the model data cannot be considered as a criterion of response predictability, but merely as a criterion of accuracy of evaluation procedures if recorded impact profiles are replaced by standardized impact profiles. In this regard it is found that the response peaks  $A_o$ ,  $A_{o1}^*$ ,  $A_{o1}$  and the respective rise times  $t_{A_o}$ , and  $t_{A_{o1}}^*$  and  $t_{A_{o1}}$  are in good accord.

## V


### RESULTS

One must be aware that the human impact tests used were designed to serve other purposes than those pursued in this study. Therefore, the results of this investigation must be presented with all reservations which might accrue from the view of adequacy of test conditions or validity of recordings or data reduction. In spite of this restriction, it was shown that:

a. The dynamic response of the chest (accelerometer) of the seated human subjected to  $+G_x$  impact can be approximated by a second or higher order system. However, the necessary trial and error variation of natural frequency  $\omega_n^*$  and damping  $\zeta^*$  during one and the same run prevent the use of (linear) spring-mass systems to predict the dynamic response of the chest (accelerometer) unless the inconsistencies in  $\omega_n^*$  and  $\zeta^*$  can be eliminated by refinement of test preparation or lawful recognition of their physical or physiological mechanics.



Table IV Comparison of Dynamic Response Data

Subject Number	Test Number	 $A_i (G_i, G_o, T)$	PHYSICAL PROPERTIES		AMPLIFICATION FACTOR	RESPONSE PEAK $G_o$			FULL $(\tau/T)$	RESPONSE PEAK $G$ FIVE TIME IN SECONDS			
			Natural Frequency $\omega_n$ RAD/SEC	$T$ SEC	Initial Damping $\zeta_i$	By Interpolation in $G_i, G_o, T$ (not shown) $\frac{A_o}{A_i}$	SIP $A_{OS}$	APPROX $A_o$		RECORDED $A_o$	SIP $t_{A_{OS}}$	APPROX $t_{A_o}$	
I	318	140	0.045	0			43	63/43	No reasonable approximation possible for any value of $\zeta_i$ = 0. Only lower response recording of 43G could be approximated.				Old Test Set Up
	335	150	0.035	0			62	66/70					Old Test Set Up
	519	130	0.046	0.2	1.51	21.2	21.5	21.5		0.46	0.023	0.027	0.042
II	319	163	0.036	0.65	1.50		36	36	0.69				Old Test Set Up
	612	145/150	0.0433	0.25	1.50	22.5	23.5	23.5	0.46	0.021	0.025	0.045	New Test Set Up
	842	134/146	0.047	0.375	1.55		31	31	0.77				New Test Set Up
III	320	140	0.045	0	1.63	23.5	40	43	0.70	0.0315	0.0325	0.0325	Old Test Set Up
	607	120/121	0.052	0.06	1.40	25.2	25	25	0.52	0.027	0.025	0.046	New Test Set Up
	755	110/114	0.057	0.25	1.40	22.5	30	29.5	0.54	0.031	0.0335	0.035	New Test Set Up
IV	332	150	0.042	0	1.49	25.4	52.5	54	0.52	0.0345	0.0315	0.0405	Old Test Set Up
	592	120	0.052	0.2	1.51	22.6	22	22	0.50	0.026	0.0295	0.0275	New Test Set Up
	606	150	0.042	0.15	1.61	25.7	27	27.5	0.52	0.022	0.0275	0.046	New Test Set Up
V	790	100	0.063	0	1.22	21.9	16	16	0.65	0.041	0.045	0.0365	New Test Set Up With Chest Parachute
	751	130	0.046	0.16	1.10		21	22	1.20		0.0575	0.0575	New Test Set Up
	846	120	0.052	0	1.60		34	33	0.50		0.0415	0.0405	New Test Set Up
VI	796	120	0.052	0.3	1.16		27	27	0.90		0.0475	0.0475	New Test Set Up With Chest Parachute
	756	110/127	0.057	0.5	1.30	26	27.5	27.5	0.49	0.026	0.025	0.031	New Test Set Up
	844	130/132	0.046	0.15	1.50		30	29	0.73		0.035	0.035	New Test Set Up

$\frac{A_o}{A_i}$  — found by interpolation in  $G_o, G_i, T$ ,  $\zeta$  (not shown in report)  $\frac{T}{T_i}$  — found by interpolation in  $G_o, G_i, \zeta$  (not shown in report)

$G_R$  Coordinate origin of recorded impact profile,  $G_{SIP}$  coordinate origin of standardized impact profile

b. The complete response coverage shown in Figures 4, 5, and 6 has proven to be an excellent means to illustrate the continuous dynamic response of the chest (accelerometer). The trial and error approximation of the complete response history established that:

1. The damping coefficient experiences a drastic change at the time of chest (accelerometer) response peak or shortly thereafter.

2. The variation of the damping coefficient  $\zeta^*$  spreading over a range from  $\zeta^* = 0$  to  $\zeta^* = 1$  seemed to be more effective than the variation of the natural frequency  $\omega_n^*$ .

3. A one second-order system was sufficient in most cases to approximate the first peak level and rise time of the dynamic chest (accelerometer) response.

c. The limited response coverages (Fig. 7 through 13) using a second-order spring-mass system can be simplified by applying standardized impact profiles. Though starting out with a different damping coefficient for different and same test subjects, the initial value of the damping coefficient  $\zeta_i^*$  was never required to be varied before the first chest (accelerometer) response peak was reached.

At first glance at the plotting of  $\omega_n^*$  versus impact peak "G" in Figure 19, it seems that the natural frequency increases with increasing impact peak "G". However, knowing that the chest instrumentation was changed for all tests subsequent to test No. 359, a confrontation of the "No. 300" test series and all subsequent tests might be misleading.

All tests subsequent to the "No. 300" test series show a difference of 40 rad/sec between the lowest and highest value of  $\omega_n^*$ . However, for one and the same test subject this difference varies from 10 to 20 rad/sec only, if the two measurements available for each subject can be considered sufficient to make this distinction.

Figure 19 illustrates the wide variation of the initial damping coefficient  $\zeta_i^*$  with reference to the response-time history limited by the response-peak onset time.

- d. It should be realized that the onset rate  $A_i/t_{A_i}$  of the impact peak is not recognizable as a parameter of autonomous significance for the investigated pulse durations up to  $2T$  (Fig. 16). If the investigator wants to consider the time element of physiological effects of impact of this duration range, it is more adequate to use the rise time of the dynamic response peak  $A_0$  since the physiological changes of impact very likely result from the change of the physical state of the body.

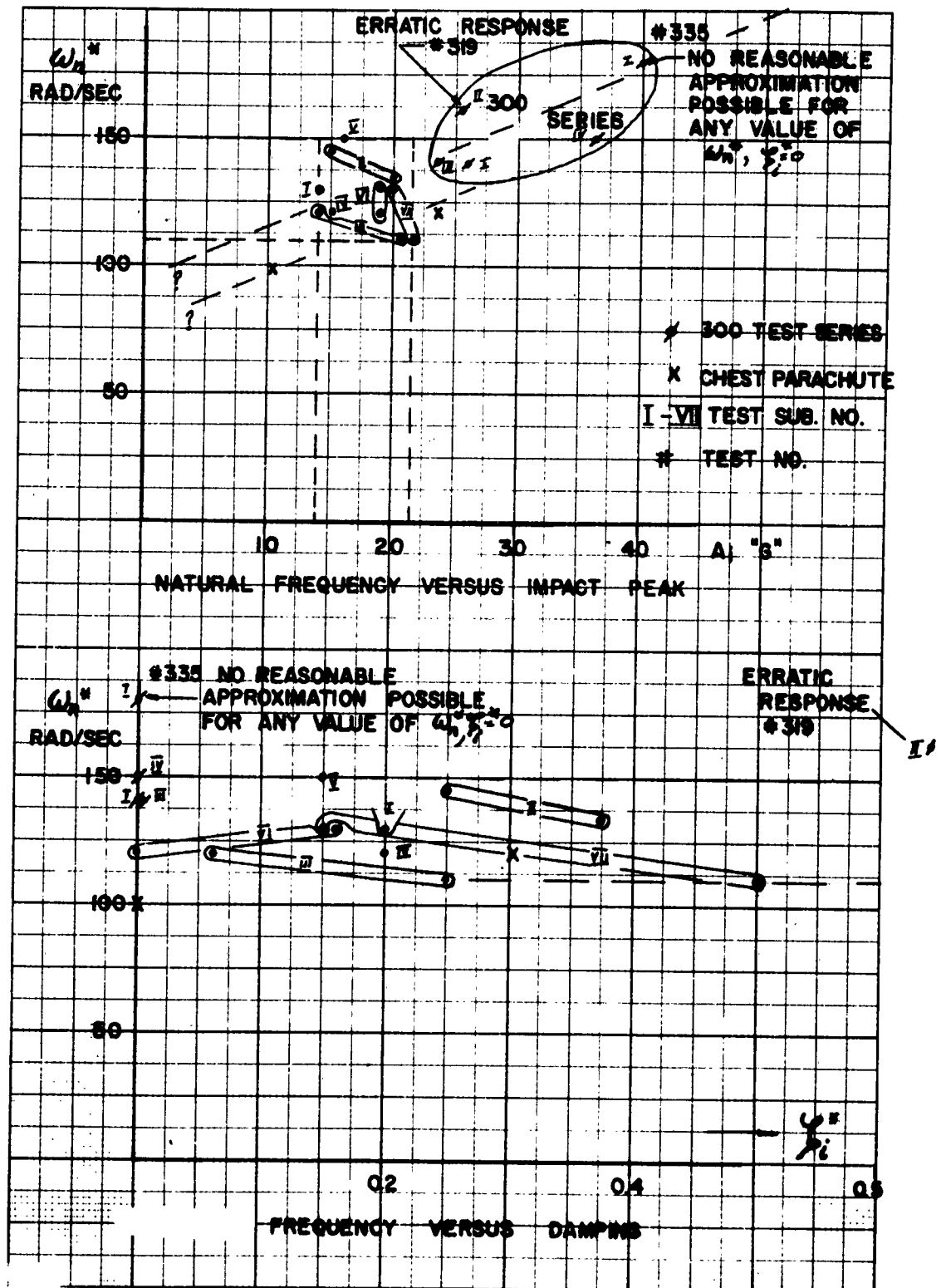


Figure 19 Dynamic Characteristic ( $\omega_n, \zeta$ ) of Humans Subjected to  $+G_x$  Impact

There is evidence that impact profiles of short enough duration will permit the development of free vibration subsequent to the transfer dynamics. The damping characteristic of the free vibration can provide for a comparison between the natural frequency of the undamped system, as established in this report, with the resonance frequency of steady state vibration as an additional means to validate the model concept chosen.

From the view of utilization of the described response analysis, it could aid the biodynamic investigator to learn by measuring at various locations, the response distribution on humans (externally) and animals (externally and internally). The simultaneous measurements at different locations would also be helpful to validate the applied evaluation procedures.

The internal instrumentation of animals can open an interesting field of simplified and informative research if the assumption of response predictability applies. Since, in this case, the momentary stress level of the body components depends directly on the dynamic behavior of the body, the inappropriate accelerometers (three components, heavy, bulky) can be replaced by absolute pressure transducers which would furnish information about the pressure history and the dynamic characteristics ( $\omega_n^*$ ,  $\zeta^*$ ) as well. In combination with the cineradiographic investigation of internal organ displacements mentioned in the introduction a well rounded test program of organ stress and strain during impact can be anticipated.

## VI

### RECOMMENDATIONS

It is recommended that additional investigations be made to validate and utilize the described trial and error approximation of the dynamic response of humans or animals subjected to impact.

From the view of validation of the assumption of the predictability of the dynamic response of the body as a whole, study continuation should concentrate on the means to improve the consistency of the model characteristics  $\omega_n^*$  and  $\zeta_i^*$  with reference to variable impact profiles. The results of this study indicate two main areas which deserve closer attention. First, the drastic change of the damping coefficient occurs at the time of the first response peak or shortly thereafter. This evidence could be related directly with the directional change of the displacement of the chest wall and consequently with the filling status of the lungs. In reverse, the difference of the filling status of the lungs at the time of impact could also explain the finding that the initial damping coefficient  $\zeta_i^*$  for the same test subject varies from test to test. A rigid control of the timing of

impact with relation to the respiratory phases could benefit the medical investigator looking at the mechanics of the physiological and pathological alterations as well as the test engineer interested in controlling the independent variables. The second area of interest is the wide spread of the natural frequency  $\omega_n^*$  of the same and of different test subjects. These differences, at least in part, could result from the mounting of the accelerometer pad to the restraint belt which was not particularly controlled in terms of restraining force and displacement. In summary, the following recommendations are made:

- a. Provide for rigid controls of respiratory function during impact in terms of timing and filling grade.
- b. Secure rigid controls of the effect of the restraint systems upon the accelerometer.
- c. Mount accelerometers at different, external locations (humans).
- d. Use pressure transducers for internal instrumentation of animals.
- e. Restrict additional program initiation to total impact duration of  $\tau < 0.5T$  to avoid the range of response overlap (Fig. 17) and to determine the characteristics of the resulting damped free vibration.

## APPENDIX

### ANALOG COMPUTER RESPONSE OF SECOND ORDER MODEL TO STANDARD IMPACT PROFILES

In the main body of this report the analog computer has been used to simulate the elastic behavior of the human body. The same computer setup was used for a parametric study of the second-order spring-mass system of the equation (2) on page 5.

The variables of the parametric evaluation are listed in Table V. The measurements are listed in Table VI.

The output measurements  $A_{O1}$ ,  $A_{O2}$ , and  $A_{O3}$  in volts are based on an input of 20 volts. Some continuous response modes are illustrated in Figures 20, 21 and 22.

Table V Symbol Chart

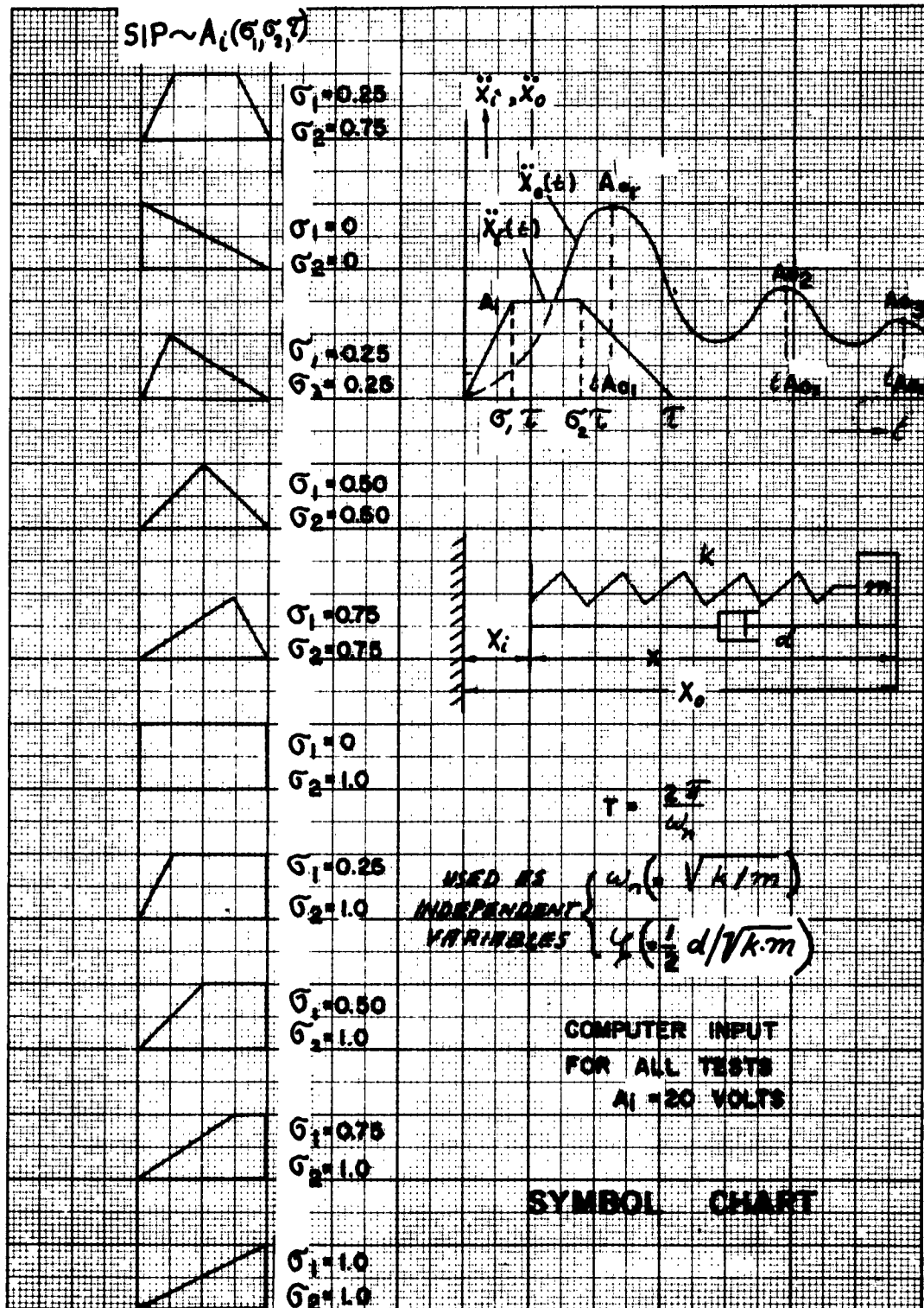


Table VI Computer Response Data of SIP

$\sigma_1$	Profile $\sigma_2$	$\tau$	Damp Coeff. $\zeta$	First response peak $A_{01}$	time $t_{A_{01}}$	Second response peak $A_{02}$	Third response peak $A_{03}$
0.25	0.75	2T	0	32.90	0.752T	30.11	25.91
0	0	2T	0	35.44	0.481T	25.18	20.36
0.25	0.25	2T	0	32.01	0.731T	18.34	17.19
0.5	0.5	2T	0	20.02	1.103T	0	0
0.75	0.75	2T	0	22.47	1.639T	17.21	17.17
0	1	2T	0	39.94	0.506T	39.92	0
0.25	1.0	2T	0	37.76	0.756T	32.75	23.17
0.5	1	2T	0	19.95	0.988T	19.92	19.92
0.75	1	2T	0	24.07	1.771T	20.21	20.21
1	1	2T	0	19.88	1.998T	19.85	19.85
0.25	0.75	T	0	38.00	0.629T	25.38	25.36
0	0	T	0	31.17	0.450T	20.23	20.23
0.25	0.25	T	0	32.51	0.575T	24.26	24.26
0.5	0.5	T	0	30.31	0.701T	25.62	25.62
0.75	0.75	T	0	25.51	0.838T	24.03	24.03
0	1	T	0	39.95	0.506T	0	0
0.25	1	T	0	38.00	0.630T	14.53	14.53
0.5	1	T	0	32.72	0.757T	23.62	23.62
0.75	1	T	0	25.95	0.892T	24.57	24.57
1	1	T	0	20.20	1.000T	20.00	20.00
0.25	0.75	T/2	0	36.03	0.503T	36.01	36.01
0	0	T/2	0	24.01	0.409T	24.78	24.78
0.25	0.25	T/2	0	25.24	0.458T	25.18	25.18
0.5	0.5	T/2	0	25.72	0.505T	25.70	25.70
0.75	0.75	T/2	0	25.08	0.505T	25.06	25.06
0	1	T/2	0	39.96	0.503T	39.96	39.96
0.25	1	T/2	0	38.72	0.533T	38.69	38.69
0.5	1	T/2	0	35.14	0.562T	35.11	35.11
0.75	1	T/2	0	29.84	0.584T	29.81	29.81
1	1	T/2	0	23.82	0.594T	23.80	23.80
0.25	0.75	T/4	0	22.08	0.381T	22.06	22.06
0	0	T/4	0	14.68	0.343T	14.67	14.67
0.25	0.25	T/4	0	14.94	0.364T	14.93	14.93
0.5	0.5	T/4	0	15.03	0.384T	15.01	15.01
0.75	0.75	T/4	0	14.88	0.405T	14.87	14.87
0	1	T/4	0	28.24	0.380T	28.22	28.22
0.25	1	T/4	0	25.31	0.396T	25.29	25.29
0.5	1	T/4	0	21.97	0.409T	21.95	21.95
0.75	1	T/4	0	18.39	0.421T	18.38	18.38
1	1	T/4	0	14.74	0.427T	14.75	14.75



(Table VI Cont'd)

Profile			Damp	First response	Second response	Third response	
$\sigma_1$	$\sigma_2$	$\tau$	Coeff. $\zeta$	peak $A_{01}$	time $t_{A_{01}}$	peak $A_{02}$	peak $A_{03}$
0.25	0.75	T/8	0	11.55	0.325T	11.55	11.55
0	0	T/8	0	7.68	0.311T	7.68	7.68
0.25	0.25	T/8	0	7.75	0.321T	7.75	7.75
0.5	0.5	T/8	0	7.77	0.331T	7.77	7.77
0.75	0.75	T/8	0	7.74	0.342T	7.74	7.74
0	1	T/8	0	15.26	0.323T	15.26	15.26
0.25	1	T/8	0	13.45	0.331T	13.45	13.45
0.5	1	T/8	0	11.57	0.340T	11.57	11.57
0.75	1	T/8	0	9.66	0.346T	9.66	9.66
1	1	T/8	0	7.75	0.352T	7.75	7.75
0.25	0.75	T/16	0	5.80	0.306T	5.80	5.80
0	0	T/16	0	3.81	0.308T	3.81	3.81
0.25	0.25	T/16	0	3.84	0.313T	3.84	3.84
0.5	0.5	T/16	0	3.93	0.300T	3.93	3.93
0.75	0.75	T/16	0	3.92	0.303T	3.92	3.92
0	1	T/16	0	7.81	0.291T	7.81	7.81
0.25	1	T/16	0	6.86	0.295T	6.86	6.86
0.5	1	T/16	0	5.89	0.300T	5.89	5.89
0.75	1	T/16	0	4.93	0.304T	4.93	4.93
1	1	T/16	0	3.96	0.308T	3.96	3.96
0.25	0.75	T/32	0	2.92	0.288T	2.92	2.92
0	0	T/32	0	1.92	0.294T	1.92	1.92
0.25	0.25	T/32	0	1.94	0.296T	1.94	1.94
0.5	0.5	T/32	0	1.94	0.299T	1.94	1.94
0.75	0.75	T/32	0	1.94	0.301T	1.94	1.94
0	1	T/32	0	3.97	0.283T	3.97	3.97
0.25	1	T/32	0	3.51	0.287T	3.51	3.51
0.5	1	T/32	0	3.00	0.289T	3.00	3.00
0.75	1	T/32	0	2.51	0.293T	2.51	2.51
1	1	T/32	0	2.02	0.299T	2.02	2.02

(Table VI Cont'd)

$\sigma_1$	Profile		Damp Coeff. $\zeta$	First response		Second response		Third response	
	$\sigma_2$	$\tau$		peak $A_{01}$	time $t_{A_{01}}$	peak $A_{02}$		peak $A_{03}$	
0.25	0.75	2T	0.15	28.36	0.731T	21.44		6.44	
0	0	2T	0.15	29.15	0.430T	10.77		2.02	
0.25	0.25	2T	0.15	27.40	0.700T	7.86		2.52	
0.5	0.5	2T	0.15	20.98	1.250T	0.49		0.10	
0.75	0.75	2T	0.15	20.83	1.589T	6.01		2.30	
0	1	2T	0.15	32.96	0.462T	24.97		6.88	
0.25	1	2T	0.15	28.35	0.732T	23.19		8.50	
0.5	1	2T	0.15	21.56	1.245T	7.97		3.05	
0.75	1	2T	0.15	22.05	1.744T	8.30		3.18	
1	1	2T	0.15	19.93	1.981T	7.94		3.07	
0.25	0.75	T	0.15	31.72	0.585T	8.86		3.42	
0	0	T	0.15	25.63	0.398T	5.06		1.96	
0.25	0.25	T	0.15	26.75	0.518T	7.10		2.75	
0.5	0.5	T	0.15	25.81	0.645T	8.45		3.27	
0.75	0.75	T	0.15	23.11	0.811T	8.77		3.38	
0	1	T	0.15	32.98	0.458T	5.00		1.94	
0.25	1	T	0.15	31.72	0.585T	6.91		2.68	
0.5	1	T	0.15	28.35	0.728T	9.35		3.62	
0.75	1	T	0.15	24.21	0.902T	9.64		3.73	
1	1	T	0.15	20.09	0.993T	7.94		3.06	
0.25	0.75	T/2	0.15	30.18	0.450T	11.74		4.52	
0	0	T/2	0.15	19.87	0.347T	7.65		2.95	
0.25	0.25	T/2	0.15	20.75	0.396T	8.05		3.11	
0.5	0.5	T/2	0.15	21.37	0.444T	8.29		3.20	
0.75	0.75	T/2	0.15	21.35	0.489T	8.23		3.18	
0	1	T/2	0.15	32.98	0.459T	13.07		5.05	
0.25	1	T/2	0.15	32.50	0.499T	12.67		4.88	
0.5	1	T/2	0.15	29.94	0.503T	11.54		4.45	
0.75	1	T/2	0.15	25.53	0.524T	9.83		3.80	
1	1	T/2	0.15	20.41	0.534T	7.87		3.04	
0.25	0.75	T/4	0.15	18.65	0.311T	7.19		2.77	
0	0	T/4	0.15	12.38	0.270T	4.78		1.83	
0.25	0.25	T/4	0.15	12.45	0.289T	4.80		1.85	
0.5	0.5	T/4	0.15	12.59	0.311T	4.85		1.87	
0.75	0.75	T/4	0.15	12.62	0.333T	4.86		1.88	
0	1	T/4	0.15	23.85	0.313T	9.19		3.56	
0.25	1	T/4	0.15	21.38	0.327T	8.24		3.18	
0.5	1	T/4	0.15	18.58	0.340T	7.14		2.77	
0.75	1	T/4	0.15	15.58	0.350T	6.02		2.32	
1	1	T/4	0.15	12.49	0.354T	4.82		1.85	

(Table VI Cont'd)

$\sigma_1$	Profile $\sigma_2$	$\tau$	Damp Coeff. $\zeta$	First response peak $A_{O1}$	time $t_{A_{O1}}$	Second response peak $A_{O2}$	Third response peak $A_{O3}$
0.25	0.75	T/8	0.15	9.79	0.248T	3.78	1.44
0	0	T/8	0.15	6.53	0.230T	2.52	0.95
0.25	0.25	T/8	0.15	6.49	0.240T	2.50	0.94
0.5	0.5	T/8	0.15	6.54	0.250T	2.53	0.95
0.75	0.75	T/8	0.15	6.58	0.261T	2.53	0.95
0	1	T/8	0.15	12.91	0.249T	4.98	1.93
0.25	1	T/8	0.15	11.38	0.256T	4.40	1.70
0.5	1	T/8	0.15	9.80	0.263T	3.80	1.47
0.75	1	T/8	0.15	8.19	0.269T	3.17	1.24
1	1	T/8	0.15	6.58	0.272T	2.55	0.98
0.25	0.75	T/16	0.15	4.92	0.214T	1.90	0.73
0	0	T/16	0.15	3.28	0.204T	1.26	0.49
0.25	0.25	T/16	0.15	3.25	0.209T	1.25	0.48
0.5	0.5	T/16	0.15	3.27	0.214T	1.26	0.49
0.75	0.75	T/16	0.15	3.31	0.218T	1.27	0.49
0	1	T/16	0.15	6.51	0.213T	2.51	0.97
0.25	1	T/16	0.15	5.71	0.217T	2.20	0.85
0.5	1	T/16	0.15	4.90	0.220T	1.89	0.73
0.75	1	T/16	0.15	4.08	0.222T	1.58	0.61
1	1	T/16	0.15	3.27	0.221T	1.26	0.49
0.25	0.75	T/32	0.15	2.47	0.196T	0.95	0.37
0	0	T/32	0.15	1.65	0.191T	0.63	0.24
0.25	0.25	T/32	0.15	1.63	0.194T	0.63	0.24
0.5	0.5	T/32	0.15	1.64	0.197T	0.63	0.24
0.75	0.75	T/32	0.15	1.65	0.199T	0.64	0.25
0	1	T/32	0.15	3.22	0.196T	1.24	0.48
0.25	1	T/32	0.15	2.78	0.198T	1.07	0.42
0.5	1	T/32	0.15	2.41	0.200T	0.93	0.36
0.75	1	T/32	0.15	2.00	0.200T	0.77	0.30
1	1	T/32	0.15	1.59	0.202T	0.60	0.23

(Table VI Cont'd)

Profile		Damp Coeff. $\zeta$	First response	Second response	Third response		
$\sigma_1$	$\sigma_2$		peak time $t_{A_{O1}}$	peak $A_{O2}$	peak $A_{O3}$		
0.25	0.75	2T	0.30	25.91	0.714T	19.80	2.31
0	0	2T	0.30	25.71	0.385T	7.57	0.48
0.25	0.25	2T	0.30	24.77	0.668T	0.66	0.10
0.5	0.5	2T	0.30	21.08	1.087T	0.62	0.10
0.75	0.75	2T	0.30	20.45	1.549T	2.41	0.35
0	1	2T	0.30	29.00	0.423T	21.24	3.32
0.25	1	2T	0.30	25.91	0.711T	20.81	3.45
0.5	1	2T	0.30	21.88	1.188T	19.76	3.32
0.75	1	2T	0.30	21.50	1.700T	3.48	0.50
1	1	2T	0.30	19.90	1.983T	3.23	0.47
0.25	0.75	T	0.30	28.12	0.544T	3.51	0.50
0	0	T	0.30	22.64	0.351T	1.41	0.21
0.25	0.25	T	0.30	23.79	0.475T	2.31	0.33
0.5	0.5	T	0.30	23.43	0.622T	3.01	0.43
0	1	T	0.30	29.00	0.422T	16.68	2.94
0.75	0.75	T	0.30	21.85	0.798T	3.33	0.47
0.25	1	T	0.30	28.12	0.554T	3.31	0.48
0.5	1	T	0.30	25.88	0.712T	3.83	0.55
0.75	1	T	0.30	23.33	0.915T	3.82	0.55
1	1	T	0.30	20.11	0.993T	3.16	0.46
0.25	0.75	T/2	0.30	27.32	0.414T	4.08	0.57
0	0	T/2	0.30	17.85	0.295T	2.63	0.38
0.25	0.25	T/2	0.30	18.76	0.345T	2.78	0.40
0.5	0.5	T/2	0.30	19.53	0.398T	2.88	0.41
0.75	0.75	T/2	0.30	19.88	0.452T	2.88	0.41
0	1	T/2	0.30	29.00	0.421T	4.60	0.66
0.25	1	T/2	0.30	28.77	0.484T	4.43	0.64
0.5	1	T/2	0.30	27.47	0.498T	4.05	0.58
0.75	1	T/2	0.30	24.26	0.498T	3.46	0.50
1	1	T/2	0.30	19.68	0.498T	2.78	0.40
0.25	0.75	T/4	0.30	17.97	0.246T	2.50	0.36
0	0	T/4	0.30	11.70	0.2171T	1.66	0.24
0.25	0.25	T/4	0.30	11.90	0.231T	1.67	0.24
0.5	0.5	T/4	0.30	12.12	0.244T	1.69	0.25
0.75	0.75	T/4	0.30	12.16	0.261T	1.79	0.25
0	1	T/4	0.30	22.97	0.251T	3.20	0.46
0.25	1	T/4	0.30	20.61	0.257T	2.87	0.42
0.5	1	T/4	0.30	17.94	0.269T	2.50	0.37
0.75	1	T/4	0.30	15.03	0.278T	2.09	0.31
1	1	T/4	0.30	12.04	0.283T	1.68	0.25

(Table VI Cont'd)

Profile		$\tau$	Damp Coeff. $\zeta$	First response peak	time	Second response peak	Third response peak
$\sigma_1$	$\sigma_2$			$A_{01}$	$t_{A_{01}}$	$A_{02}$	$A_{03}$
0.25	0.75	T/8	0.30	9.38	0.174T	1.29	0.18
0	0	T/8	0.30	6.24	0.153T	0.86	0.12
0.25	0.25	T/8	0.30	6.20	0.163T	0.85	0.12
0.5	0.5	T/8	0.30	6.25	0.173T	0.86	0.12
0.75	0.75	T/8	0.30	6.28	0.184T	0.86	0.12
0	1	T/8	0.30	12.39	0.175T	1.71	0.24
0.25	1	T/8	0.30	10.90	0.181T	1.51	0.21
0.5	1	T/8	0.30	9.38	0.188T	1.30	0.18
0.75	1	T/8	0.30	7.82	0.193T	1.08	0.15
1	1	T/8	0.30	6.27	0.195T	0.87	0.12
0.25	0.75	T/16	0.30	4.76	0.147T	0.66	0.09
0	0	T/16	0.30	3.16	0.131T	0.44	0.06
0.25	0.25	T/16	0.30	3.13	0.136T	0.43	0.06
0.5	0.5	T/16	0.30	3.16	0.141T	0.44	0.06
0.75	0.75	T/16	0.30	3.17	0.154T	0.44	0.06
0	1	T/16	0.30	6.30	0.142T	0.87	0.12
0.25	1	T/16	0.30	5.53	0.145T	0.77	0.11
0.5	1	T/16	0.30	4.74	0.149T	0.66	0.09
0.75	1	T/16	0.30	3.95	0.151T	0.55	0.08
1	1	T/16	0.30	3.15	0.153T	0.44	0.06
0.25	0.75	T/32	0.30	2.38	0.135T	0.331	0.05
0	0	T/32	0.30	1.59	0.121T	0.220	0.03
0.25	0.25	T/32	0.30	1.57	0.124T	0.218	0.03
0.5	0.5	T/32	0.30	1.58	0.126T	0.220	0.03
0.75	0.75	T/32	0.30	1.59	0.129T	0.221	0.03
0	1	T/32	0.30	3.11	0.126T	0.428	0.06
0.25	1	T/32	0.30	2.69	0.128T	0.374	0.06
0.5	1	T/32	0.30	2.29	0.129T	0.319	0.05
0.75	1	T/32	0.30	1.89	0.131T	0.264	0.04
1	1	T/32	0.30	1.50	0.131T	0.209	0.03

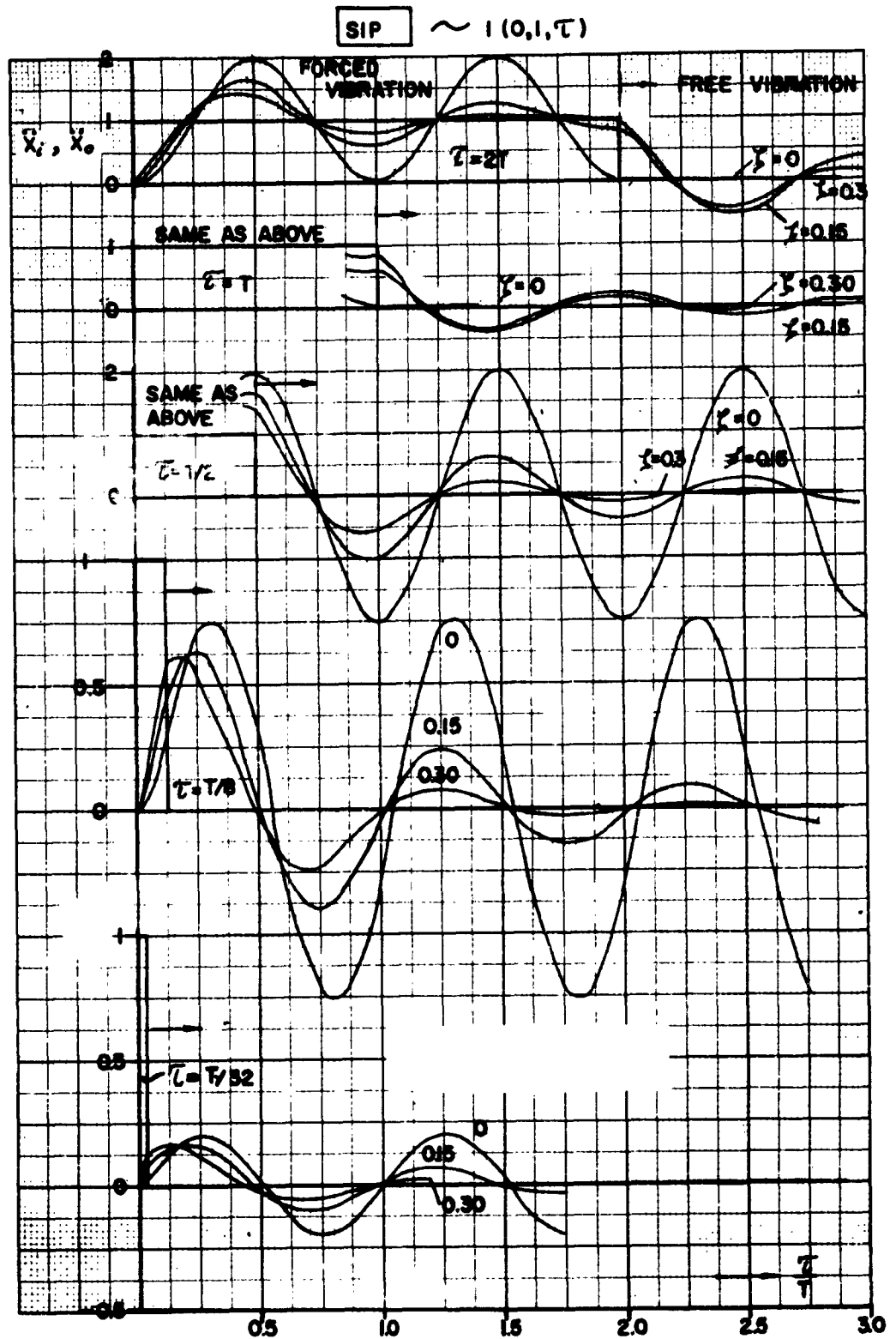


Figure 20 Continuous Response Modes of SIP (Rectangular Profile)

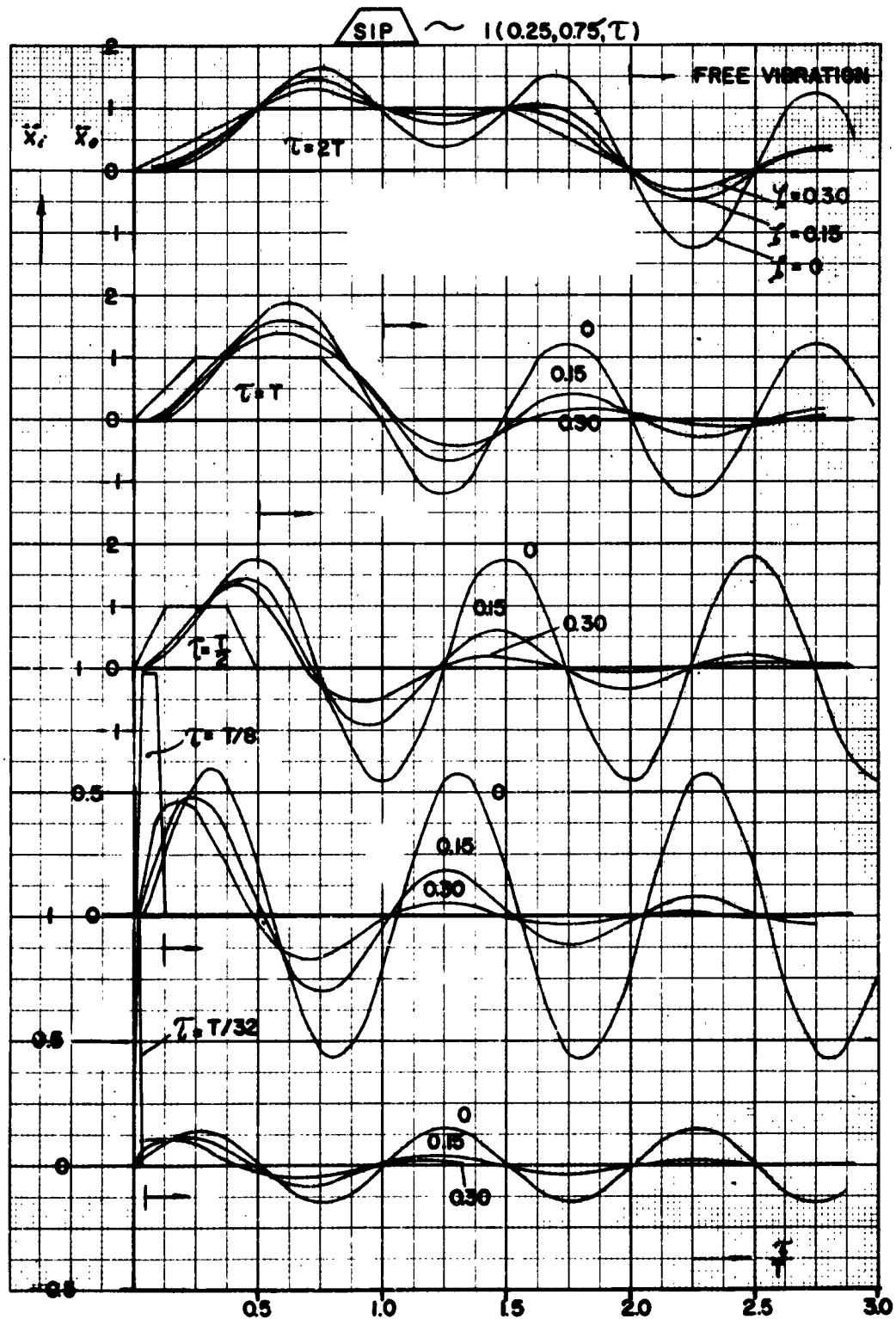


Figure 21 Continuous Response Modes of SIP (Trapezoidal Profile)

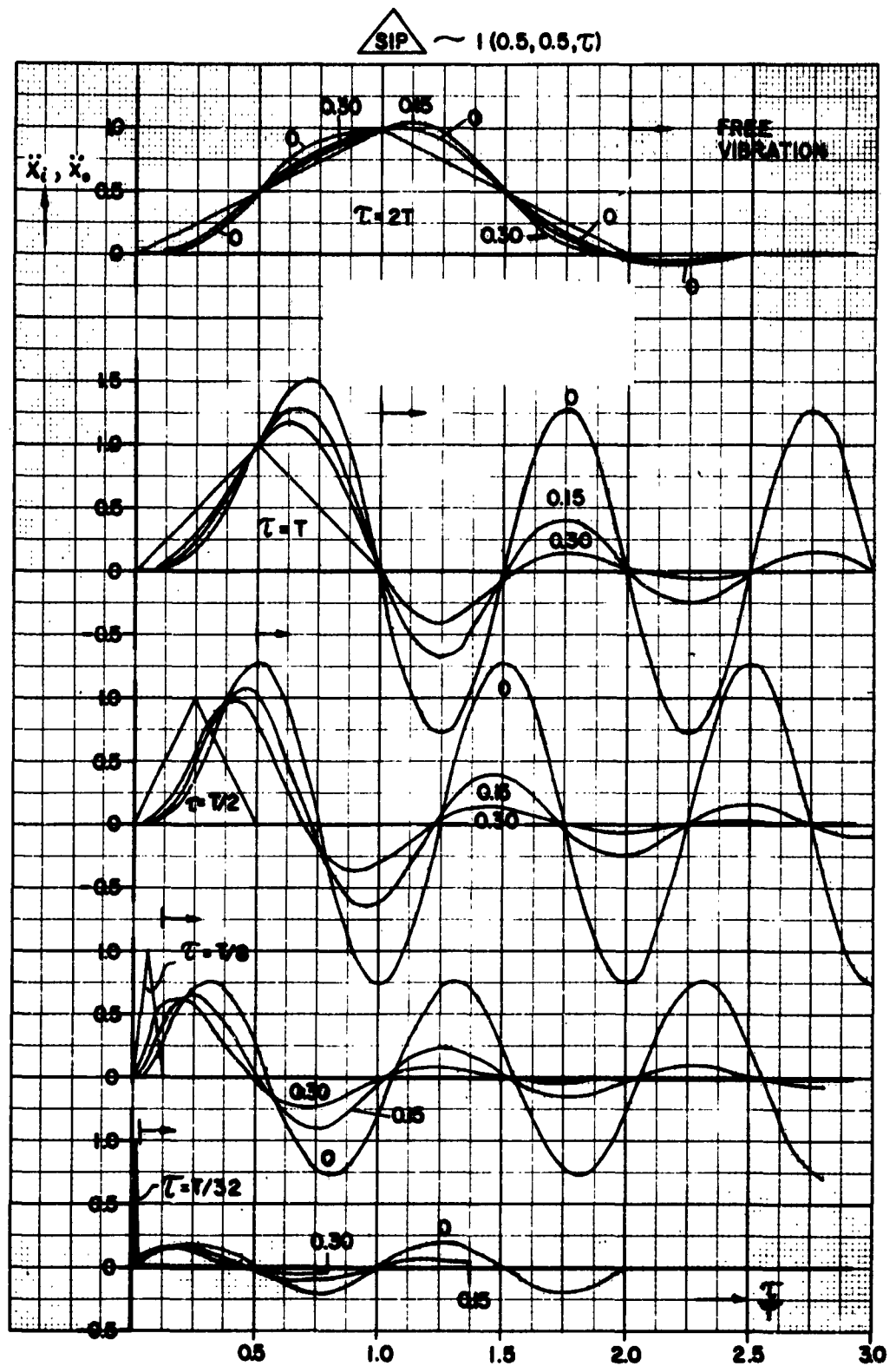


Figure 22 Continuous Response Modes of SIP (Triangular Profile)



Unclassified

Security Classification

DOCUMENT CONTROL DATA - R&D		
(Security classification of title, body of abstract and indexing annotation must be entered when the overall report is classified)		
1 ORIGINATING ACTIVITY (Corporate author)		2a REPORT SECURITY CLASSIFICATION
6571st Aeromedical Research Laboratory		Unclassified
		2b GROUP
3 REPORT TITLE		
DYNAMIC RESPONSE ANALYSIS OF +G <sub>x</sub> IMPACT ON MAN		
4 DESCRIPTIVE NOTES (Type of report and inclusive dates)		
Interim		
5 AUTHOR(S) (Last name, first name, initial)		
Feder, Hubert C. and Root, E. H.		
6 REPORT DATE	7a TOTAL NO OF PAGES	7b NO OF REFS
November 1964	52	0
8a CONTRACT OR GRANT NO.	9a. ORIGINATOR'S REPORT NUMBER(S)	
b PROJECT NO 7231	ARL-TR-64-11	
c Task 723106	9b. OTHER REPORT NO(S) (Any other numbers that may be assigned this report)	
d		
10 AVAILABILITY/LIMITATION NOTICES		
11 SUPPLEMENTARY NOTES	12. SPONSORING MILITARY ACTIVITY	
	6571st Aeromedical Research Laboratory Holloman AFB, New Mexico	
13 ABSTRACT		
<p>An analog computer was used to compare the dynamic response of an accelerometer placed over the sternum of human test subjects during impact in +G<sub>x</sub> direction with the response of second and higher order spring-mass systems. Identity of the response modes of both systems, human and mechanical, was approximated by trial and error modification of natural frequency and damping coefficient of the computer model used. With restriction to only a few cases investigated and to the particular test conditions, best compliance of complete response coverage is considered to result from the application of a single spring-mass system of irregularly varying damping coefficient. A parametric analysis of the single spring-mass system is presented to aid the use of standardized impact profiles. The usefulness of the method of response approximation has been established, but the validation of the underlying concept of response predictability needs further investigation.</p>		

DD FORM 1473  
1 JAN 64

Unclassified

Security Classification

16. KEY WORDS	LINK A		LINK B		LINK C	
	ROLE	WT	ROLE	WT	ROLE	WT
Man Impact Dynamic response Accelerometer Spring-mass systems						

#### INSTRUCTIONS

1. **ORIGINATING ACTIVITY:** Enter the name and address of the contractor, subcontractor, grantee, Department of Defense activity or other organization (*corporate author*) issuing the report.

2a. **REPORT SECURITY CLASSIFICATION:** Enter the overall security classification of the report. Indicate whether "Restricted Data" is included. Marking is to be in accordance with appropriate security regulations.

2b. **GROUP:** Automatic downgrading is specified in DoD Directive 5200.10 and Armed Forces Industrial Manual. Enter the group number. Also, when applicable, show that optional markings have been used for Group 3 and Group 4 as authorized.

3. **REPORT TITLE:** Enter the complete report title in all capital letters. Titles in all cases should be unclassified. If a meaningful title cannot be selected without classification, show title classification in all capitals in parenthesis immediately following the title.

4. **DESCRIPTIVE NOTES:** If appropriate, enter the type of report, e.g., interim, progress, summary, annual, or final. Give the inclusive dates when a specific reporting period is covered.

5. **AUTHOR(S):** Enter the name(s) of author(s) as shown on or in the report. Enter last name, first name, middle initial. If military, show rank and branch of service. The name of the principal author is an absolute minimum requirement.

6. **REPORT DATE:** Enter the date of the report as day, month, year, or month, year. If more than one date appears on the report, use date of publication.

7a. **TOTAL NUMBER OF PAGES:** The total page count should follow normal pagination procedures, i.e., enter the number of pages containing information.

7b. **NUMBER OF REFERENCES:** Enter the total number of references cited in the report.

8a. **CONTRACT OR GRANT NUMBER:** If appropriate, enter the applicable number of the contract or grant under which the report was written.

8b, 8c, & 8d. **PROJECT NUMBER:** Enter the appropriate military department identification, such as project number, subproject number, system numbers, task number, etc.

9a. **ORIGINATOR'S REPORT NUMBER(S):** Enter the official report number by which the document will be identified and controlled by the originating activity. This number must be unique to this report.

9b. **OTHER REPORT NUMBER(S):** If the report has been assigned any other report numbers (*either by the originator or by the sponsor*), also enter this number(s).

10. **AVAILABILITY/LIMITATION NOTICES:** Enter any limitations on further dissemination of the report, other than those

imposed by security classification, using standard statements such as:

- (1) "Qualified requesters may obtain copies of this report from DDC."
- (2) "Foreign announcement and dissemination of this report by DDC is not authorized."
- (3) "U. S. Government agencies may obtain copies of this report directly from DDC. Other qualified DDC users shall request through \_\_\_\_\_."
- (4) "U. S. military agencies may obtain copies of this report directly from DDC. Other qualified users shall request through \_\_\_\_\_."
- (5) "All distribution of this report is controlled. Qualified DDC users shall request through \_\_\_\_\_."

If the report has been furnished to the Office of Technical Services, Department of Commerce, for sale to the public, indicate this fact and enter the price, if known.

11. **SUPPLEMENTARY NOTES:** Use for additional explanatory notes.

12. **SPONSORING MILITARY ACTIVITY:** Enter the name of the departmental project office or laboratory sponsoring (*paying for*) the research and development. Include address.

13. **ABSTRACT:** Enter an abstract giving a brief and factual summary of the document indicative of the report, even though it may also appear elsewhere in the body of the technical report. If additional space is required, a continuation sheet shall be attached.

It is highly desirable that the abstract of classified reports be unclassified. Each paragraph of the abstract shall end with an indication of the military security classification of the information in the paragraph, represented as (TS), (S), (C), or (U).

There is no limitation on the length of the abstract. However, the suggested length is from 150 to 225 words.

14. **KEY WORDS:** Key words are technically meaningful terms or short phrases that characterize a report and may be used as index entries for cataloging the report. Key words must be selected so that no security classification is required. Identifiers, such as equipment model designation, trade name, military project code name, geographic location, may be used as key words but will be followed by an indication of technical context. The assignment of links, rules, and weights is optional.

## DISTRIBUTION

<b>AFSC (SCTB)</b> <b>Andrews AFB</b> <b>Wash, DC 20331</b>	<b>2</b>	<b>Academy Library-DFSLB</b> <b>United States Air Force Academy</b> <b>Colorado 80840</b>	<b>2</b>
<b>Hq USAF, Science Division</b> <b>(AFRSTA)</b> <b>Dir/Science and Technology,</b> <b>DCS/R&amp;D</b> <b>Wash, DC 20330</b>	<b>1</b>	<b>American Institute of Aero-</b> <b>navitics and Astronautics</b> <b>750 Third Avenue,</b> <b>New York, NY 10017</b>	<b>1</b>
<b>AMD</b> <b>ATTN: Chief Scientist</b> <b>Brooks AFB, Texas 78236</b>	<b>1</b>	<b>Boeing Airplane Company</b> <b>Aero-Space Division</b> <b>ATTN: Ruth E. Peerenboom</b> <b>P. O. Box 3707</b> <b>Seattle, Wash 98124</b>	<b>1</b>
<b>AMD (AMAP)</b> <b>Brooks AFB, Texas 78236</b>	<b>10</b>	<b>Redstone Scientific Information</b> <b>Center</b> <b>ATTN: Chief, Document Section</b> <b>U. S. Army Missile Command</b> <b>Redstone Arsenal, Ala 35809</b>	<b>5</b>
<b>DDC (TIAAS)</b> <b>Cameron Station</b> <b>Alexandria, Va 22314</b>	<b>20</b>	<b>British Liaison Office</b> <b>Army Missile Test and Evalu-</b> <b>ation Directorate</b> <b>White Sands Missile Range</b> <b>New Mexico 88002</b>	<b>1</b>
<b>AFETR Tech Library (MU-135)</b> <b>Patrick AFB, Fla 32922</b>	<b>1</b>	<b>Defence Research Member</b> <b>Canadian Joint Staff</b> <b>Director of Biosciences Research</b> <b>2450 Massachusetts Ave., N. W.</b> <b>Wash, DC 20008</b>	<b>1</b>
<b>APGC (PGBAP-1)</b> <b>Eglin AFB, Fla 32542</b>	<b>1</b>	<b>USAF School of Aerospace</b> <b>Medicine</b> <b>ATTN: Aeromedical Library</b> <b>Brooks AFB, Texas 78236</b>	<b>1</b>
<b>ESD (ESTI)</b> <b>L. G. Hanscom Field</b> <b>Bedford, Mass 01730</b>	<b>2</b>	<b>Life Sciences Dept., Code N300</b> <b>U. S. Naval Missile Center</b> <b>Point Mugu, Calif 93041</b>	<b>1</b>
<b>Air University Library</b> <b>Maxwell AFB, Ala 36100</b>	<b>1</b>		
<b>6570th AMRL (MRRSL, Library)</b> <b>WPAFB, Ohio 45433</b>	<b>2</b>		
<b>Central Intelligence Agency</b> <b>ATTN: OCR/DD-Standard</b> <b>Distribution</b> <b>Wash, DC 20505</b>	<b>2</b>		

Aviation Medical Acceleration Laboratory ATTN: AMAL Library Johnsville, Pa 18974	2	Medical Records Section Room 325 Division of Medical Sciences National Academy of Sciences National Research Council 2101 Constitution Avenue NW Wash, DC 20418	1
Librarian C.A.R.I. F.A.A. P.O. Box 1082 Oklahoma City, Okla 73101	1	Aviation Safety Engineering Research A Division of Flt Safety Foundation 2871 Sky Harbor Blvd Sky Harbor Airport Phoenix, Arizona 85034	1
Director U.S. Naval Research Laboratory (Code 5360) Wash, DC 20390	2	NASA Langley Research Center Langley Station ATTN: Librarian MS 185 Hampton, Va 23365	3
Biomedical Library Center for Health Sciences University of California Los Angeles, Calif 90024	1	Archive-Library Dept American Medical Assoc 535 N. Dearborn St., Chicago, Ill., 60610	1
Technical Reference Library U.S. Naval Medical Research Institute Bethesda, Md 20014	1	Information Officer USAFE French Liaison Office Det 0100, 7260th Support Group APO New York, NY 09686	1
Director Walter Reed Army Institute of Research ATTN: Neuropsychiatry Division Wash, DC 20012	1	The Decker Corp 45 Monument Road Bala-Cynwyd, Pa 19004	1
Commanding Officer (Code 373) U.S. Naval School of Aviation Medicine U.S. Naval Aviation Medical Center Pensacola, Fla 32512	2	Douglas Aircraft Co., Advance Biotechnology Dept Missile and Space Systems Div Santa Monica, Calif 90406	1
Dr. W.M. Helvey 0/55-60 B/151 Lockheed Missiles and Space Co P.O. Box 504 Sunnyvale, Calif 94088	1	Literature Acquisition Dept Biological Abstracts 3815 Walnut St Philadelphia, Pa 19104	1

The Lovelace Foundation 1  
Dept of Aerospace Medicine and  
Bioastronautics  
5200 Gibson Boulevard, S.E.  
Albuquerque, NMex 87108

Dr. William D. Thompson 1  
Department of Psychology  
Baylor University  
Waco, Texas

Institute of Laboratory Animal 1  
Resources  
National Academy of Sciences/  
National Research Council  
2101 Constitution Ave., N.W.  
Wash, DC 20037

Dr. Deets Pickett 1  
8505 Lee Blvd  
Leawood, Kansas 66206

Dr. Walter J. Frajola 1  
M-351 Starling-Loving Hall  
Ohio State University  
Columbus 10, Ohio 43210

Dr. R.D. Gafford 1  
Project Manager, Space Engineering  
Beckman Instruments, Inc  
2500 Harbor Blvd  
Fullerton, Calif 92632

Commanding Officer 1  
U.S. Naval Medical Field Re-  
search Laboratory  
ATTN: Library  
Camp Lejeune, NC

Aerospace Medicine Bibliog- 1  
raphy Project  
Science and Technology Division  
Library of Congress  
Wash, DC 20540

Dr. F.H. Rohles 1  
Institute for Environmental  
Research  
Kansas State University  
Manhattan, Kansas

Mr. Elliott H. Morse 1  
Librarian  
Library of the College of  
Physicians of Philadelphia  
19 South 22nd Street  
Philadelphia, Pa 19103

Dr. Leon H. Schmidt, Director 1  
National Center for Primate  
Biology  
University of California  
Davis, Calif 95616

Del Electronics Corp 1  
Research and Development Dept  
ATTN: Leonard R. Solon, Ph.D.  
250 E. Sandford Blvd.,  
Mount Vernon, New York

Civil Aeromedical Research 1  
Institute  
Federal Aviation Agency  
Aeronautical Center  
ATTN: John N. Ice, Am-119  
Editor, Acceleration Project  
P.O. Box 1082  
Oklahoma City, Okla 73101

Director 1  
Flyvemedicinsk Institute  
Copenhagen, Denmark

National Aeronautics and Space 2  
Administration  
Scientific and Technical Infor-  
mation Facility  
ATTN: NASA Representative  
Bethesda, Md 20014

Human Research Branch 2  
 (Code RBH)  
 OART, NASA Headquarters  
 Wash, DC 20546

HQ, U.S. Army Medical R&D 1  
 Command  
 ATTN: Chief, Behavioral Sciences  
 Research Branch  
 Room 2608, Main Navy Bldg.,  
 Washington, DC 20315

Local

MDNH 1  
 NLO 1  
 ARGS 80  
 RRRT 3  
 RRRS 1